# ULTRASONIC WAVE PROPAGATION IN POLY(VINYL ALCOHOL) HYDROGELS AND ARTICULAR CARTILAGE

A Thesis
Presented to
The Academic Faculty

By

Hsingching Crystal Hsu

In Partial Fulfillment
Of the Requirements for the Degree
Master of Science in Mechanical Engineering

Georgia Institute of Technology

July 2004

# ULTRASONIC WAVE PROPAGATION IN POLYVINYL ALCOHOL HYDROGELS AND ARTICULAR CARTILAGE

Approved by:

Dr. Yves Berthelot, Advisor

Dr. Marc Levenston, Advisor

Dr. Robert Guldberg

July 2, 2004

ACKNOWLEDGEMENT

I would like to thank my advisors for their help and advice throughout the course of this research. Dr. Marc Levenston and Dr. Yves Berthelot provided direction that guided me to accomplish this project and I am very grateful for their incredible support. Thanks to them, I have learned so much about acoustics, ultrasonics, cartilage biomechanics and bioengineering.

I would also like to thank the graduate students in both labs I worked in. They were always willing to help offer advice and answer questions. I would like to thank Stacy Imler and Chris Wilson for taking the time to teach me how to use various lab equipment. I would also like to thank Valerie Sitterle for her advice in ultrasonics and hydrogel manufacturing, and Onyi Irrechukwu for her patient explanations of various bioengineering topics.

Finally, I would like to thank my parents and sister for their support and providing motivation to finish my research.

TABLE OF CONTENTS

LIST OF TABLES

LIST OF FIGURES

# SUMMARY

AN ultrasonic nondestructive evaluation (NDE) technique has been developed to characterize the superficial layer of articular cartilage. The technique utilizes the unique properties of surface waves to detect changes in mechanical properties of the surface layer of the test sample. Experiments were performed first on poly(vinyl alcohol) (PVA) hydrogels, a material used to model articular cartilage, to examine repeatability and the ability of wave propagation parameters to reflect changes in material properties. Dynamic shear and compression tests were performed on 20% and 25% PVA by weight hydrogels to examine the difference in material properties. Ultrasonic NDE tests with longitudinal, shear and surface waves were performed on the hydrogels. Wave speeds in the 20% and 25% hydrogels were compared. Results showed that ultrasonic NDE with surface waves was repeatable and the technique was able to detect material property changes in hydrogels. Ultrasonic NDE tests with surface waves were then performed on healthy and damaged bovine articular cartilage. Wave speeds in the healthy cartilage were compared to speeds in enzymatically digested cartilage. Results showed that ultrasonic NDE with surface waves was repeatable and the technique was able to detect material property changes in the superficial layer of articular cartilage. Findings suggest that the technique has potential to be a tool in diagnosing diseases involving cartilage degeneration, such as osteoarthritis.

# CHAPTER 1

# INTRODUCTION

Osteoarthritis (OA) is a degenerative disease that progressively destroys cartilage on articulating joints. Cartilage degeneration begins with collagen denaturation. This early stage of degeneration causes degradation of the matrix and a deformation throughout the cartilage thickness, which contribute to the progressive destruction of the entire tissue and loss of joint function.[1] Since OA is characterized by damage in the superficial collagen matrix before detectable cartilage destruction begins, detecting changes in the material properties of the superficial layer would be extremely beneficial in studies of OA treatment and prevention. Such a tool could potentially become a clinical instrument for arthroscopic diagnosis of OA or for monitoring progression and treatment of the disease.

Ultrasonic nondestructive evaluation (NDE) testing methods are used extensively in purely mechanical systems for material characterization.[2] NDE techniques have also been applied to biological tissues. There have been many studies investigating ultrasound propagation of longitudinal waves in articular cartilage.[35, 36, 37] Ultrasound propagation properties of wave speed and attenuation depend on the tissue structure, and differences in these parameters reflect changes in material properties of cartilage. These studies typically use transmission configurations, which propagate the acoustic wave through the entire layer of cartilage. The characterization of the whole thickness cannot detect the changes of the superficial layer that would indicate the early stages of degeneration in OA. In this thesis, a novel approach is developed to study the changes of

the superficial layer in cartilage. Instead of using bulk waves, surface (Rayleigh) waves are used in ultrasonic NDE methods. Surface waves are a class of guided acoustic waves that propagate along the surface of a material. By measuring the properties of surface wave propagation in cartilage, it is hypothesized that the superficial layer of cartilage can be characterized by analyzing the wave speed and attenuation.

To investigate the ability of ultrasonic surface waves to characterize the surface of a test material, experiments on poly (vinyl alcohol) (PVA) hydrogels and articular cartilage were performed. Initial tests were performed on PVA hydrogels, a model material for cartilage, to prove the novel technique could be used on a biphasic material. Surface wave contact transducers were used to demonstrate that a surface wave could be generated in the hydrogel. After successful surface wave generation, a series of surface wave measurements were taken to demonstrate repeatability of surface wave generation in hydrogels. Finally, surface wave measurements were performed on PVA hydrogels of different mechanical properties to investigate the sensitivity of surface wave properties to differences in material properties of the hydrogel.

The same procedure was applied to articular cartilage. Surface contact transducers were used to demonstrate surface wave generation is possible and repeatable in healthy cartilage. Ultrasonic NDE methods with surface waves were then applied to damaged cartilage to investigate the sensitivity of surface wave properties to changes in mechanical properties of the superficial layer in articular cartilage. Surface wave speeds and attenuation in healthy cartilage were compared to speeds and attenuation in damaged cartilage.

# CHAPTER 2

# BACKGROUND

## *2.1 Articular cartilage*

Articular cartilage is a soft tissue lining the articulating surfaces of diarthroidal joints. Cartilage provides a low friction bearing surface for smooth joint articulation. Cartilage also acts as a shock absorber by distributing joint loads to decrease peak contact stresses in joints.[3] Its porous-permeable nature is important for joint lubrication. The physiological mechanical functions of cartilage are possible because of its composition, matrix ultrastructure, and the complex interactions between its constituents.

### *2.1.1 Composition of articular cartilage*

Cartilage is composed of a collagen fiber matrix interspersed with proteoglycans and inflated by interstitial fluid. Based on wet weight, articular cartilage is primarily made of ionized interstitial fluid (70% - 85%), collagen (10% - 20%), proteoglycans (5-10%), with other quantitavely minor constituents.[5] Its physical behavior has been modeled as a biphasic (fluid and solid) and triphasic (fluid, solid, ionic) material based on continuum mixture theory or poroelasticity.[5] Mature cartilage is relatively acellular, containing only one cell type, the chondrocyte. Because of the small amount of cells and a lack of blood vessels, cartilage has a low level of metabolic activity compared to tissues such as muscle or bone.[1]

The primary type of collagen in articular cartilage is collagen type II. The collagen fibers form a matrix network with a specific ultrastructural organization that

gives cartilage its form and stability. Collagen has a high tensile stiffness which contributes to the ability of cartilage to withstand tensile and shear stresses.

The most abundant type of proteoglycan in articular cartilage is aggrecan.[4] Aggrecan consists of glycosaminoglycan (chondroitin and keratin sulfate) chains connected to a protein core. The aggrecan molecule binds to a hyaluronic acid core to form negatively charged macromolecular aggregates.[5] The aggregates interact with the positively charged ionic interstitial fluid which causes a significant osmotic swelling pressure. This interaction contributes to the tissue's ability to withstand sustained compressive stresses.

Other interactions between cartilage constituents are also a factor in the biomechanical function of the tissue. The osmotic swelling stress from the proteoglycan-fluid interaction allows cartilage to resist shear stress.[5] Swelling stress in cartilage is also affected by the restriction of proteoglycans by the collagen network. The proteoglycans and collagen network give the tissue its low permeability to make cartilage resistant to fluid flow under compressive loads. When subjected to rapid or cyclic compressive loading (i.e. walking and other functional daily activities), the low permeability produces an apparent stiffening of cartilage.[6]

### *2.1.2 Structure of articular cartilage*

Cartilage is organized in a zonal organization.[7] The superficial or tangential zone is at the articulating surface of the joint. Below is the upper radial (middle), then the lower radial (deep) zone, and finally calcified cartilage/subchondral bone. (Figure 1) Based on weight, collagen and water content is highest at the surface and decreases with depth while proteoglycan content is lowest at the surface and increases with depth.[8] The

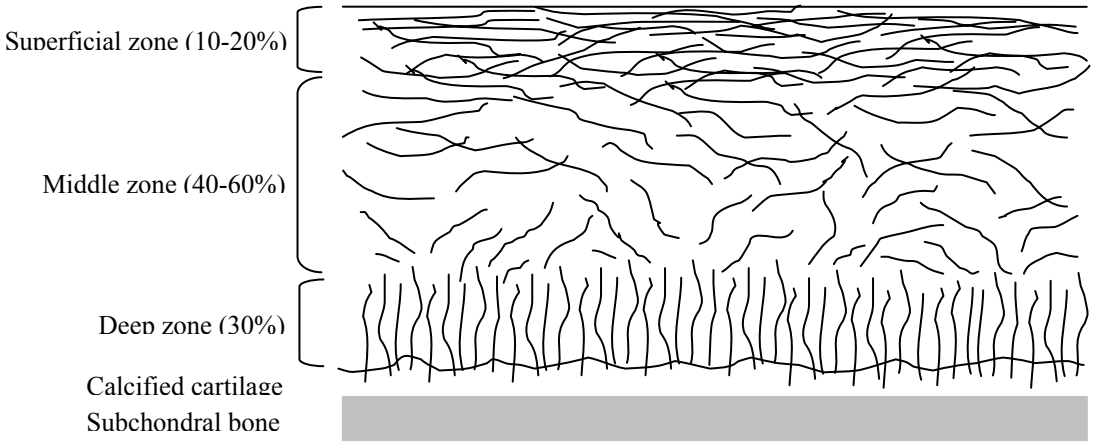


Figure 1: Zonal organization of articular cartilage illustrating the predominant collagen orientation in each zone[5]

collagen network radially extends from the subchondral bone in the lower radial (deep) zone to anchor cartilage to the subchondral bone. In the middle zone, collagen has a random organization[3]. At the superficial zone, the collagen network is tangentially. The different organization of each zone allows each to respond differently to mechanical loading and have specialized functions within the tissue.

*2.1.3 Superficial zone*

The superficial zone occupies only 10%-20% of the total cartilage thickness.[9] The collagen fibrils are oriented tangentially (parallel to surface) and there is low proteoglycan and cell content. Within the plane of the superficial zone, the collagen orientation varies with position on the joint surface. Though the exact relationship is uncertain, the predominant fibrillar orientation can be seen with "split lines" that can be generated by puncturing the cartilage surface with a fine pin.[10]

The unique structure and composition of the superficial layer give it specific mechanical properties. The dense collagen network gives the superficial zone a high

tensile stiffness and resistance to shear stresses. The superficial zone has a low equilibrium compressive modulus though it exhibits the greatest amount of stiffening with increasing compression relative to the other zones. This is caused by the increased tensile strain of the superficial zone under compression which leads to an apparent stiffening due to the high tensile stiffness of collagen.[11] The superficial zone also contributes to the compressive behavior of the entire tissue. The collagen network in the superficial layer restricts fluid flow through the joint surface, which contributes to the swelling pressure that allows cartilage to resist compressive loads.[12] In addition, the compressive modulus of the superficial zone increases dramatically with increasing compressive strain.[13] The unique properties of the superficial layer help to limit deformation through the bulk of the tissue by protecting the cells and the tissue matrix.

### *2.1.4 Mechanical properties of articular cartilage*

The composition and structural complexity of articular cartilage make it very difficult to fully characterize the mechanical properties of the tissue. The zonal architecture and various collagen orientation throughout cartilage makes the tissue anisotropic and inhomogeneous. Cartilage exhibits stress relaxation and creep behavior. Under a constant load, fluid within cartilage flows and the height of the articular surface decreases until equilibrium is reached. Under a constant deformation, fluid in cartilage is pressurized causing a high initial stress. The stress gradually decreases and reaches equilibrium as fluid flows and redistributes within the matrix.[1,5] High water content and the collagen matrix give cartilage its poro-viscoelastic nature.

Several constitutive models and testing methods have been used to characterize cartilage. The most widely used is the biphasic theory, which was developed by Mow

and his coworkers.[5] Confined compression and biphasic indentation experiments are used to obtain expressions for the properties of cartilage. In confined compression, samples are compressed in a chamber preventing lateral expansion and allowing uninhibited fluid flow from the tissue. Biphasic indentation uses an indenter to apply compressive loads on a sample and a numerical parameter estimation procedure to determine material constants. With theses two testing methods, a number of studies have reported elastic compression modulus values for cartilage. Athanasiou, et al., reported an average modulus of 0.63 MPa for human femoral chondyles.[14] Mow, et al., reported an average modulus of 0.45 MPa for bovine articular cartilage.[15] Jurvelin, et al., reported an average modulus of 0.58 MPa for canine femoral chondyle cartilage.[16]

Shear properties of cartilage are typically determined with pure shear experiments under small strain conditions. This eliminates volumetric change and hydrodynamic pressures so interstitial fluid cannot flow in the cartilage.[17] In the experiment, a cylindrical sample is subjected to torsional shear deformation. The average equilibrium shear modulus for human patellar cartilage was found to be 0.23 MPa.[18] The equilibrium shear modulus for canine femoral condylar cartilage was found to be 0.22 MPa.[19]

The tensile modulus of cartilage has been determined from equilibrium data of stress relaxation experiments.[20] For healthy cartilage, the equilibrium stress-strain relationship is linear for strains up to 15%.[5] The equilibrium tensile modulus is determined in this linear region. Various studies have shown wide range of values for the tensile modulus. The equilibrium tensile modulus for the superficial layer of the bovine humerus was found to be 13.4 ± 4.6 MPa.[21] The equilibrium tensile modulus for the superficial layer of the human femoral groove and condyle was found to be 13.9 ± 2.4

MPa and 7.8 ± 1.7 MPa respectively.[22] The variation is due to the different type of joints, different animals, location on the joint, depth from the surface, and other factors.

*2.1.5 Osteoarthritis*

Osteoarthritis (OA) is a common joint disease affecting a majority of adults over the age of 65 years.[23] OA is a gradual but progressive degradation of the cartilage extracellular matrix that eventually leads to joint failure. The disease begins with cartilage surface roughening, followed by fibrillation, and then macroscopic fissuring and complete loss of bony coverage in advanced cases.[24] Clinical symptoms typically include joint stiffness and pain, and can progress to partial or complete immobilization.[25] A common risk factor is mechanical trauma from overuse, direct trauma or injury to other soft tissues.[26] Biochemical changes include loss of proteoglycans and an increase in pro-inflammatory cytokines, which lead to matrix degradation.[27] This damage to the structural integrity of cartilage causes further cell-mediated degradation, creating a progressive cycle of degradation and causing adverse changes in the cartilage material properties. In a canine ACL transaction model, there was a 44% decrease in tensile stiffness due to structural changes in the superficial zone.[28] The tensile modulus of human OA tissue is over 80% lower than that of normal tissue near the surface.[29]

Several studies of human OA and animal models indicate that denaturation of superficial zone cartilage may be one of the earliest changes in the development of OA. In experimental lapine arthritis induced by external patellar trauma, cell death and changes to the collagen fibrillar structure began in the superficial zone.[30] In mice with a collagen IX mutation, erosion of the surface was seen as the first sign of this genetically

linked OA.[31] In human OA, the greatest level of collagen II denaturation was seen in the superficial zone.[32]

## *2.2 Current cartilage testing methods*

To determine cartilage material properties, many studies use mechanical testing methods such as compression, shear and tension tests. These methods destroy the joint surface for sample preparation, which make them not feasible for studies of small animal joints. Recently, a novel osmotic swelling technique has been developed for indirectly measuring the inhomogeneous tensile stiffness of articular cartilage.[33] Bath solution salinity in a full thickness tissue sample is decreased to induce osmotic swelling. A confocal microscope is then used to see the two dimensional deformation throughout the sample. The tensile stiffness is calculated using a Donnan swelling model and proteoglycan content measurement from adjacent tissue. This technique provides information on the depth dependent tensile properties of the small animal joints; however, the method depends on an appropriate model for osmotic swelling and properties in only one surface direction (in the plane of the tissue slab) can be determined. In addition, the joint is destroyed for sample preparation.

### *2.2.1 Nondestructive testing methods*

The most common nondestructive test of cartilage mechanical properties is the indentation test.[16] The indentation test has been used extensively to study mechanical properties of cartilage in a variety of large animal models as well as small animals. Although a common test, determining material properties from the indentation test can be difficult, especially for joints with thin cartilage and a high curvature. Indenter geometry

and consistent placement on the joint surface can dramatically change the apparent stiffness.[34] Also, thickness of the cartilage layer being investigated depends on the indenter size. Indenters with diameters on the order of the cartilage thickness determine mechanical properties of the full thickness. Smaller indenters provide more information about surface properties but the method inherently involves deeper layers in the mechanical response.[11] The sensitivity of the method to the indenter does not make indentation testing an ideal method for detecting changes in the superficial zone.

*2.2.2 Ultrasonic nondestructive evaluation*

Ultrasonic nondestructive evaluation (NDE) is a class of techniques using ultrasonic wave propagation to characterize the mechanical properties of a material. Several types of waves are used in ultrasonic NDE, including longitudinal (compression) waves, shear (transverse) waves, and surface (Rayleigh) waves. Longitudinal waves are acoustic waves in which the particle motion is in the same direction as the wave propagation. (Figure 2)

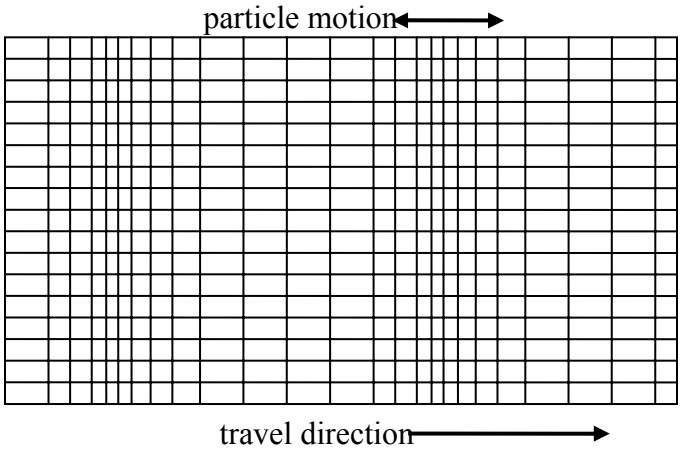


Figure 2: Particle motion of a longitudinal wave

For homogeneous, isotropic materials the longitudinal wave speed, $C_L$, is given by

$$C_L = \sqrt{\frac{\lambda + 2\mu}{\rho}},$$

where λ and μ are the Lamé constants and ρ is the material density.

Shear waves are acoustic waves in which the particle motion is perpendicular to the direction of wave propagation. (Figure 3)

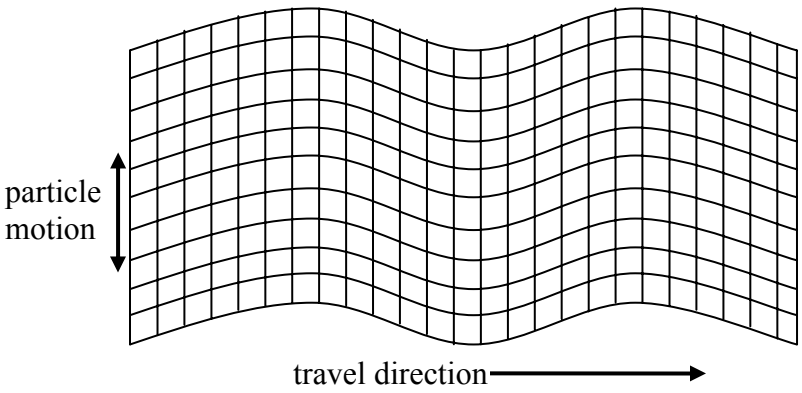


Figure 3: Particle motion of a shear wave

Shear wave speed, $C_S$, is given by

$$C_S = \sqrt{\frac{\mu}{\rho}},$$

where μ is the shear modulus of the material and ρ is the material density. Longitudinal and shear waves involve propagation of a compressive or shear deformation through the bulk of the medium, while Rayleigh waves involve propagation along a free surface.

Wave speed and attenuation are parameters typically used to describe ultrasound propagation through materials. Wave speeds do not depend on frequency for an ideal, non-dispersive, purely elastic medium; however, all biological tissues are dispersive and

therefore have some frequency dependence. Attenuation is a measure of the degradation in signal strength (amplitude) or energy (proportional to the square of the amplitude) as a wave travels through the material. As with wave speed, attenuation is frequency dependent for a dispersive medium. The dispersion of a medium can be determined by examining the frequency dependence of ultrasound speed and attenuation.

The majority of ultrasonic measurements in biological tissues (including cartilage) involve pulse echo techniques with longitudinal wave propagation. An ultrasonic wave source is placed on the test material and generates a longitudinal wave. When the wave encounters a surface, part of the incident wave is reflected back and part of the wave is transmitted through the medium (Figure 4). At the opposite surface, part of the transmitted wave passes through the interface and part of it will reflect back as backscatter.

By analyzing the properties of the different waves, mechanical properties of the sample can be determined. Techniques such as scanning acoustic microscopy (SAM) and scanning laser acoustic microscopy (SLAM) analyze the transmitted wave. Scanning backscatter microscopy (SBM) uses the reflected and backscattered waves to characterize the test material. Backscatter techniques can be used to analyze articular cartilage since the method would be nondestructive.

A number of studies have shown that ultrasonic longitudinal wave propagation reflects changes in matrix composition and structure of articular cartilage. Testing at 100 MHz, Agemura, et al., found that attenuation significantly increases when intermolecular cross links were broken in collagen and waves propagate more rapidly across collagen fibrils than along them.[35]

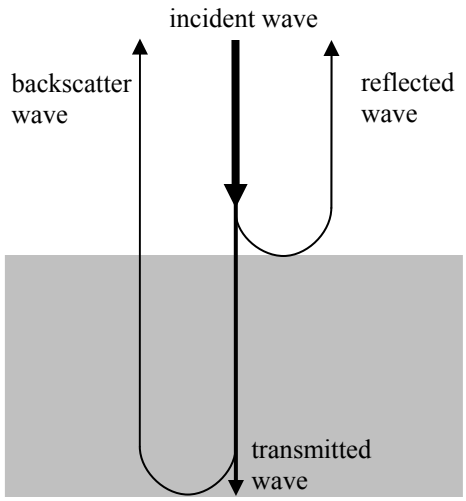


Figure 4: Transmission and reflection modes in ultrasonic NDE

Pellaumail, et al., analyzed rat patellae with a scanning backscatter microscope in the 28-79 MHz bandwidth.[36] Their findings indicate wave speed and attenuation decrease with collage fiber density. Nieminen, et al., tested real time degradation of bovine cartilage at 29.4 MHz and found attenuation increased after trypsin digestion.[37] The increase in attenuation is believed to be caused by the cleavage of collagen links from the digestion. Toyras, et al., found wave velocity to decrease after collagenase and chondroitinase digestion suggesting proteoglycans depletion causes a lower wave velocity.[38] Senzig, et al., reported that attenuation was higher in regions identified as weight bearing areas on femoropatellar groove cartilage.[39] Damage to the cartilage surface can also influence ultrasonic measurements. The backscatter power increases with abrasion induced surface roughness, with similar effects observed for osteoarthritic cartilage. Acoustic reflection from the cartilage surface decreases with increased surface roughness and the progression of osteoarthritis.

Cartilage composition and properties affect longitudinal ultrasonic wave propagation through cartilage; however, backscatter measurements determine properties of the full cartilage thickness and reflection measurements reflect roughness of the articular surface. While nondestructive in nature, ultrasonic NDE techniques using bulk waves cannot characterize only the superficial layer of cartilage.

*2.2.2.1 Rayleigh waves*

Unlike longitudinal and shear waves, Rayleigh waves are guided waves, which propagate at large distances along a free surface. In the late 19$^{th}$ century, Lord Rayleigh was the first to propose the existence of a wave that can propagate along a stress free surface but its amplitude exponentially decays with depth. To satisfy the stress free boundary condition, the longitudinal and shear displacements combine at the surface into an elliptical motion (Figure 5).

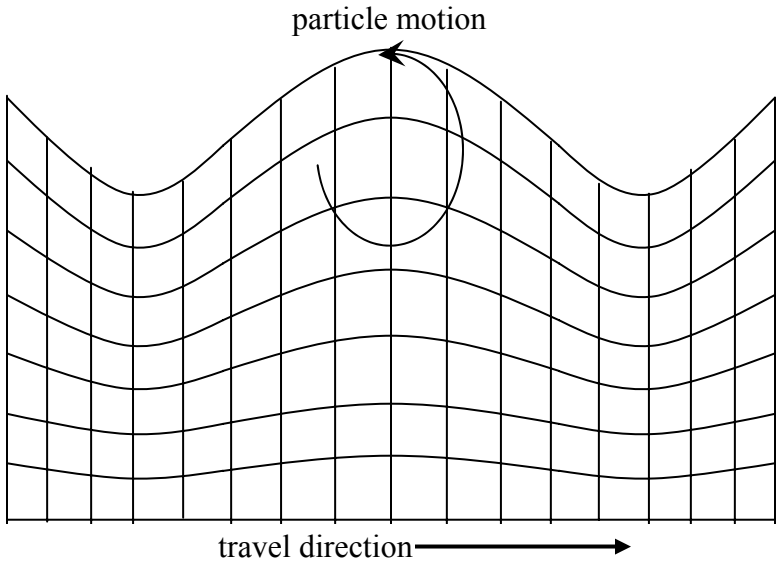


Figure 5: Particle displacement motion of Rayleigh wave propagation on a surface

In an isotropic, homogeneous medium, Rayleigh waves travel at approximately 90% of the shear wave velocity.[40] Rayleigh wave speed, $C_R$, is given by

$$C_R = \sqrt{\frac{\mu}{\rho}}\left(\frac{0.87+1.12\nu}{1+\nu}\right),$$

where μ is the shear modulus of the material, ρ is the material density, and ν is the Poisson's ratio.

The depth of penetration is approximately one wavelength below the surface, so Rayleigh waves are ideal for characterizing the mechanical properties of the surface layer of a medium. Rayleigh waves are frequently used in nondestructive evaluation applications, not only to characterize the surface material properties but also to detect flaws and defects. At low frequencies, Rayleigh waves are used in earthquake monitoring[41], to assess the integrity of aging pavements and runways[42], and to detect buried landmines.[43] At ultrasonic frequencies, Rayleigh waves are used to monitor the growth of small cracks in samples under cyclical loading[44], to characterize surface roughness[45] or to measure mechanical properties in various materials.[46] In addition to characterizing a material's surface layer, layers of different thickness can be probed by changing the frequency of the Rayleigh wave. At higher frequencies, the wavelengths are short and the wave is confined to a small layer near the surface. At lower frequencies, the wavelength is longer and the layer being investigated is thicker.

Ultrasonic NDE using surface waves is best suited for investigating changes in the superficial layer of cartilage, because the method is nondestructive and the use of surface waves focuses on characterizing the surface layer and not the entire tissue.

*2.2.2.2 Rayleigh waves on curved surfaces*

Rayleigh waves are also able to propagate along smooth curved surfaces almost unhindered.[47] The general case of a smooth curved surface satisfies the condition $k\rho_{min} \gg 1$, where k is the Rayleigh wave number and $\rho_{min}$ is the minimal radius of curvature. The radii of curvature on orthogonal lines are given by $\rho_u$ and $\rho_v$, where u and v are a system of local Cartesian coordinates (Figure 6).

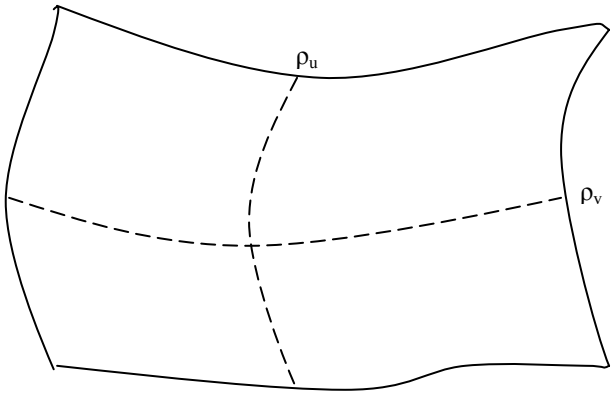


Figure 6: Smooth curved surface of arbitrary form with a local system of coordinates

The wave speed, c, of a Rayleigh wave on a curved surface is given by

$$c = c_o(1+\eta), \qquad \eta = a_u \frac{1}{k_o \rho_u} + a_v \frac{1}{k_o \rho_v}$$

where $c_o$ is the Rayleigh wave velocity on a plane surface, $k_o$ is the Rayleigh wave number for a plane surface, and $a_u$ and $a_v$ are given by

$$a_u = -\frac{A}{2B}, \qquad a_v = -\frac{G}{2B}.$$

The constants A, B and G depend on wave numbers of longitudinal, shear, and Rayleigh waves (see Appendix A). Assuming the radii of curvature on the bovine tibial plateau are

typically greater than 15 mm, the η term would be very small and thus the Rayleigh wave speed on a curved surface, c, would be very close to the Rayleigh wave speed on a plane surface. This illustrates that the curvature of the tibial plateau would have a negligible effect on Rayleigh wave speed measurements.

*2.2.2.3 Rayleigh wave models*

There are many models of Rayleigh wave propagation in complex materials. Destrade modeled Rayleigh wave propagation in orthotropic incompressible elastic materials.[48] The material axes of the body are denoted by $x_1$, $x_2$, and $x_3$ where $x_2$ is the depth. He focuses on surface waves that are subsonic relative to homogeneous body waves. The surface is assumed to be free of tractions and assumption of plane strain is not required. The secular equation derived is given as

$$(C_{11} + C_{22} - 2C_{12} - \rho v^2)^2 (C_{66} - \rho v^2) = C_{66} (\rho v^2)^2,$$

where $C_{11}$, $C_{22}$, $C_{12}$, and $C_{66}$ are the stiffness constants, ρ is the material density, and v is the Rayleigh wave speed for waves propagating in the $x_1$ direction. For waves propagating in the $x_3$ direction, $C_{11}$ is replaced by $C_{33}$, $C_{12}$ is replaced by $C_{23}$, and $C_{66}$ is replaced by $C_{44}$. It is interesting to note that the predicted Rayleigh waves are non-dispersive.

Ogden and Vinh built upon Destrade's model by deriving a secular equation for Rayleigh waves in incompressible orthotropic elastic solids that does not admit spurious solutions.[49] With the same assumptions, the Rayleigh wave speed, v, propagating in the $x_1$ direction is given as

$$\frac{\rho v^2}{\gamma} = 1 - \frac{1}{9}\left( -1 + \sqrt[3]{\frac{9\Delta + 16 + 3\sqrt{3}\sqrt{4\Delta^2 - 13\Delta + 32}}{2}} + \sqrt[3]{\frac{9\Delta + 16 - 3\sqrt{3}\sqrt{4\Delta^2 - 13\Delta + 32}}{2}} \right)^2 ,$$

where ρ is the material density, γ is $C_{66}$, and Δ is defined as

$$\Delta = \frac{C_{11} + C_{22} - 2C_{12}}{C_{66}} .$$

Royer and Dieulesaint derived a secular equation for Rayleigh waves propagating in a compressible orthotropic elastic material which is given by:

$$C_{22}C_{66}\zeta^2(C_{11} - \zeta) = (C_{66} - \zeta)[(C_{22}(C_{11} - \zeta) - C_{12}^2]^2 , \qquad \zeta = \rho v^2$$

where $C_{11}$, $C_{22}$, and $C_{66}$ are the stiffness constants, ρ is the material density, and v is the Rayleigh wave speed.[50]

Several studies have investigated the propagation of surface waves on gels. Kikuchi, et al., studied surface waves ranging from 20 Hz to 800 kHz on agarose gels.[51] From the dispersion curve of the gel, it was seen that surface tension (and not elasticity as is usually the case in standard materials) is the dominant restoring force mechanism for frequencies higher than 20 kHz, indicating that the gel surface behaves like a liquid above 20 kHz. The phase velocity, v, of the surface wave is given by

$$v = \sqrt[3]{\frac{2\pi\sigma}{\rho} f} ,$$

where ρ is the material density, σ is the surface tension, and f is frequency of the surface wave. Above 20 kHz, phase velocities in gelatin and agarose gels were found to be on the order of 5 m/s. Matsuoka, et al., studied surface tension wave and Rayleigh waves in crosslinked polyacrylate hydrogels in the frequency range of 1100 to 2000 Hz.[52] The coexistence of the two modes (elastic and surface tension) was not observed, and it was

concluded that the Rayleigh mode was predominant based on amplitude measurements. The Rayleigh wave speed, v, was estimated as

$$v = \sqrt{\frac{0.91G}{\rho}},$$

where ρ is the material density and G is the gel rigidity. Assuming rubber elasticity, G is given as

$$G = \upsilon kT\phi^{1/3}\phi_o^{2/3},$$

where υ is the number of crosslinked chains per unit volume of dry gel, k is the Boltzmann constant, T is the temperature, φ is the volume fraction of the gel, $\varphi_o$ is the volume fraction of the network at the condition at which polymer chains have random-walk configurations. For gels with a water content higher than 60%, velocities ranged from 4 – 10 m/s.

Takashi, et al., studied surface waves at 250-750 Hz in gelatin solution and models surface wave propagation to have characteristics of both surface tension waves and Rayleigh waves.[53] When both surface tension and elasticity are taken into account, the surface wave velocity, v, is given as

$$v^2 = \frac{\gamma k}{\rho} + \frac{0.91G}{\rho},$$

where ρ is the material density, γ is surface tension, k is the wave number, and G is the shear elasticity of the gel.

*2.2.2.4 Contact transducers*

To generate the acoustic waves, contact transducers are used for ultrasonic NDE methods. Contact transducers used in this study have a piezoelectric material (PZT) as

their active elements to convert electrical energy, such as an excitation pulse, into ultrasonic energy. The piezoelectric material can also pick up ultrasonic energy and convert it to electrical energy. The active element is cut to specifically produce longitudinal or shear waves. To generate a surface wave, angle beam (surface wave) transducers use the principles of refraction and mode conversion to produce refracted longitudinal or shear waves in the test material. The piezoelectric contact transducer generates a longitudinal wave that travels through an angled wedge. At the boundary of the wedge and the test material, some energy from the incident longitudinal wave is transmitted to the test material. The transmitted waves are a shear and longitudinal wave that propagates at an angle different from the incident angle, based on refraction and mode conversion. (Figure 7)

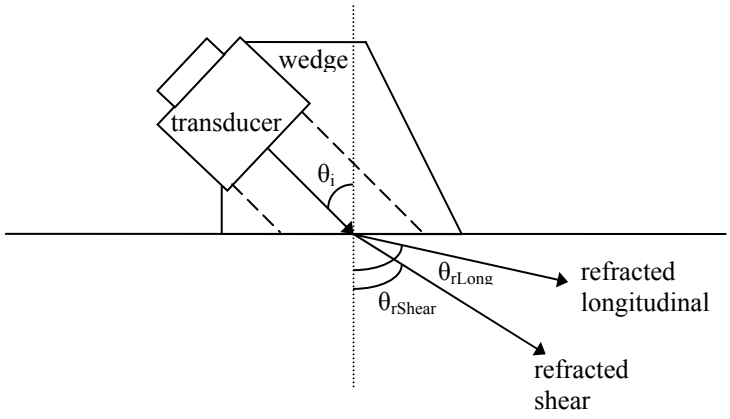


Figure 7: Refracted longitudinal and shear waves from angle beam transducer

The incident angle needed to produce a desired refracted wave can be calculated using Snell's law. The law states

$$\frac{\sin\theta_i}{C_i} = \frac{\sin\theta_r}{C_r},$$

where $\theta_i$ is the incident angle of the wedge, $\theta_r$ is the angle of the refracted wave, $C_i$ is the wave speed in the wedge, and $C_r$ is the wave speed in the test material.

To produce a surface wave, the incident angle of the wedge is increased until the refracted longitudinal and shear waves are propagating at the surface. The incident angle of the built-in wedge in the angle beam (or surface wave) transducers used in this study is 65°.

### ***2.3 PVA hydrogels***

Poly (vinyl alcohol) (PVA) hydrogels are a promising biomaterial that has potential to replace articular cartilage. PVA hydrogels are a cross-linked network of hydrophilic polymers that can absorb up to thousands of times their dry weight in water.[54] Depending on the PVA concentration, PVA hydrogels can be developed to have 60% - 90% water content. Hydrogels are not homogeneous, since groups of molecular entanglements can create inhomogeneities. Free chain ends or chain loops can also cause network defects. During the manufacturing process, trapped air bubbles and skin formation on the surface can also contribute to inhomogeneities in the hydrogel. Properties of PVA hydrogels include high water content, low permeability, biocompatibility, viscoelasticity, biphasic nature, and low coefficient of friction. PVA hydrogels also exhibit desirable mechanical and swelling properties.

Several studies have been performed to test the mechanical properties of PVA hydrogels. Peppas, et al., crosslinked PVA hydrogels with irradiation and strengthened the material with a heat annealing process.[55, 56] They reported the material to have tensile modulus ranging from 5.16 – 9.35 MPa and an ultimate strength of 1.72-11.03 MPa with elongation at break of 200% - 300%. Sasada, et al., crosslinked PVA hydrogels with the

freeze/thaw process to create hydrogels with 80 – 90% water content.[57] They reported an elastic modulus of approximately 1 MPa and ultimate stress of 1-10 MPa. Researchers in Kyushu University of Japan also used an iterative freeze/thaw process to develop a hydrogel of 79% water content.[58, 59] They reported an elastic modulus of 1.1 MPa. Gu, et al., also used an iterative freeze/thaw process and irradiation to develop a hydrogel that had a tensile strength ranging from 2.23 – 4.47 MPa and compressive moduli ranging from 8.99 – 14.84 MPa.[60] Stammen, et al., used the freeze/thaw iterative process to develop hydrogels and found compressive moduli to range from 1.1 to 18.4 MPa, failure stress to be 2.1 MPa, and shear modulus to range from 0.17- 0.43 MPa for hydrogels that are 75% water.[61]

Having properties and a structure similar to cartilage, PVA hydrogels are used in this study as a model material for articular cartilage. Ultrasonic NDE tests with surface waves are performed on PVA hydrogels first to demonstrate proof of concept on a visco-poroelastic, hydrated, inhomogeneous material. Besides being a simpler material, PVA hydrogels are more manageable since the geometry is easily controlled by dictating the dimensions of the molds. PVA hydrogel material properties can also be controlled by dictating the PVA concentration and the water content. Use of a non-biological material also eliminates variability from biological degradation and sample to sample variability.

# CHAPTER 3

# MATERIAL CHARACTERIZATION OF PVA HYDROGELS

## ***3.1 Method of making PVA hydrogels***

To make a hydrogel, a solution of poly(vinyl alcohol) (PVA) and deionized water was poured into a mold and then subjected to two cycles of freezing and thawing. The PVA polymer chains were thermally cross-linked when the solution went through freeze/thaw cycles. The amount of cross linking increases with more freeze/thaw cycles.

First, dry PVA powder was mixed with deionized water. The PVA powder used was 99+% hydrolyzed with an average molecular weight of 124,000-186,000 supplied by Sigma Aldrich Incorporated. Two mixture ratios of PVA and deionized water were used: 20% PVA by weight and 25% PVA by weight. To form the 20% PVA solution, 37.5 grams of PVA was mixed with 150 mL of deionized water. For the 25% PVA solution, 50 grams of PVA was mixed with 150 mL of deionized water. The mixtures were autoclaved at 220°C for 20 minutes to force the PVA into solution.

Then, the solutions were placed in an oven at 100°C for 30 minutes to allow air bubbles to escape from the solution. This minimized air pocket formation in the body of the hydrogels after pouring the solutions into the molds. Two different shapes of plastic molds were used. One mold is 3.524 in by 3.524 in by 0.579 in (89.5 mm by 89.5 mm by 14.7 mm) and the other is 5 in by 3.252 in by 0.315 in (127.0 mm by 82.6 mm by 8.0 mm). The PVA solutions were slowly poured into the molds. An aluminum sheet 0.125 in (3.175 mm) thick was placed over the molds and clamped to another 0.125 in aluminum sheet underneath the molds. The 20% PVA and 25% PVA solutions were

frozen at -20°C for eight hours and thawed at roomed temperature (20°C) for eight hours. This freeze/thaw cycle was repeated twice. The finished hydrogels were removed from the molds and stored in deionized water at room temperature until time of testing.

### ***3.2 Dehydration rate of hydrogels***

An experiment to determine the dehydration rate of the hydrogels was performed to ensure no significant water loss during the expected time of a NDE experiment. The hydrogels were weighed at room temperature every fifteen minutes for one and a half hours. The initial weight of the 20% and 25% hydrogels were 27.68 g and 27.15 g respectively. Over 90 minutes, the 20% hydrogel lost water at a rate of 0.0108 g/min and the 25% gel lost water at 0.0103 g/min. The dehydration rate was minimal relative to the initial weight of the hydrogels, though water loss was probably from the hydrogel surfaces. It was assumed that water loss due to dehydration is not likely a major factor affecting change of surface wave speeds during ultrasonic NDE testing.

### ***3.3 Mechanical testing on hydrogels***

To determine the quasi-static material properties of the hydrogels, dynamic shear and compression tests were performed. Cylindrical hydrogel samples 0.236 in (6 mm) in diameter and 0.157 in (4 mm) thick were punched out of the 5 in by 3.252 in by 0.315 in molds with a 6 mm biopsy punch. Three cylindrical samples each of 20% and 25% hydrogels were used in the mechanical tests. Dynamic shear tests were performed using a Bohlin rheometer (model CVO120HR). Sandpaper (Al oxide 100 grit) was glued to the platen and base to provide better contact with the hydrogel samples. The base was filled with deionized water to keep the hydrogel sample hydrated during the experiment. The

platen was lowered to have a static offset of 10% of the initial sample height. The geometrical setting was chosen to be 6mm parallel plate for shear moduli calculations. Shear tests were performed at 0.01Hz and 0.1Hz at 0.05% strain with a nine second delay time. Results from the shear tests are listed in Table 1.

Table 1: Complex shear moduli of 20% and 25% PVA hydrogel samples

| Sample # | Frequency (Hz) | 20% PVA shear modulus (Pa) | 25% PVA shear modulus (Pa) |
|---|---|---|---|
| 1 | 0.01 | 85,577 | 159,290 |
| 2 | 0.01 | 71,896 | 195,500 |
| 3 | 0.01 | 64,802 | 187,440 |
| Average | | **74,092** | **180,743** |
| St. dev | | **10,560** | **19,482** |
| | | | |
| 4 | 0.1 | 87,371 | 161,220 |
| 5 | 0.1 | 74,112 | 199,550 |
| 6 | 0.1 | 67,208 | 186,450 |
| Average | | **76,230** | **182,407** |
| St. dev. | | **10,247** | **19,011** |

The two sample t-test statistical analysis was used to compare the shear moduli of the 20% and 25% hydrogel at the two frequencies. At 0.01 Hz, it was found that the shear moduli of the 20% and 25% hydrogels were significantly different ($p = 0.003$). The average shear modulus of the 25% hydrogel was 244.0% higher than the average shear modulus of the 20% hydrogel. At 0.1 Hz, it was found that the shear moduli of the 20% and 25% hydrogels were significantly different ($p = 0.004$). The average shear modulus of the 25% hydrogel was 239.3% higher than the average shear modulus of the 20% hydrogel.

Dynamic unconfined compression tests were performed using the EnduraTec ELF 3200. A 25 N load cell was attached to a well to hold the hydrogel samples. The hydrogel samples were placed in the well, which was filled with deionized water. The samples underwent stress relaxation at 5%, 10%, 15%, and 20% strain with a ramp rate of 1 mm/sec. The hold time at the 5% and 10% strain was eight minutes, and the hold time for 15% and 20% strain was ten minutes. Results from the compression test are listed in Table 2.

Table 2: Equilibrium compressive moduli of 20% and 25% PVA hydrogel samples

| Sample # | 20% PVA Modulus (Pa) | 25% PVA Modulus (Pa) |
|---|---|---|
| 1 | 439,900 | 853,000 |
| 2 | 368,700 | 956,000 |
| 3 | 413,600 | 1,013,100 |
| Average | **407,400** | **940,700** |
| St. Dev | **36,003** | **81,139** |

Using a two sample t-test statistical analysis, it was found that the equilibrium compressive moduli of the 20% and 25% hydrogels were significantly different ($p = 0.009$). The average compressive modulus of the 25% hydrogel was 230.9% higher than the average compressive modulus of the 20% hydrogel.

Though the dynamic mechanical tests were not performed at the frequencies of the ultrasonic NDE tests, the mechanical tests were used to demonstrate a significant difference in material properties between the 20% and 25% hydrogels.

### *3.4 Protocol for measuring surface wave speed*

Before ultrasonic NDE testing began, a protocol for measuring ultrasonic surface wave speeds was established to ensure repeatability from testing procedures. The sample was tested in air at room temperature. A pair of Panametrics surface wave transducers 0.65 in by 0.31 in by 0.40 in (16.51 mm by 7.87 mm by 10.16 mm) was placed on the test material surface to generate and detect a surface wave on the sample. The transducers used were either 2.25 MHz (model number A564S-RM) or 5 MHz (model number A574S-RM). The transducer has an area of contact with samples of 0.65 in by 0.31 in (16.51 mm by 7.87 mm). Propylene glycol couplant was used on the transducers to conduct the acoustic waves between transducer and sample. A piece of floss with marked incremental distances was placed on the sample surface alongside the transducers. The source transducer remained stationary as the receiver transducer was placed along the sample surface in incremental distances by aligning the transducer with the markings on the floss. The transducers were connected to a 25 MHz bandwidth pulser-receiver (Panametrics 500PR) with BNC to microdot transducer cables. The pulser-receiver was attached to a digital oscilloscope (Tektronix TDS 420A), which recorded wave signals at a sampling rate of 200 MHz. The signals were analyzed to find the time of arrival of the received wave packet. The time of arrival of the received wave signal was measured for several distances between the transducers, and the surface wave speed was calculated by taking the slope of distance versus the time of arrival plot. A run was defined as the data taken over a range of incremental distances to calculate the surface wave speed. Typically, several runs were made and then surface wave speeds were averaged.

*3.4.1 Time of arrival*

There were several specific points on the received signal that could be taken as the time of arrival. In this study, the time of arrival was taken to be the start of the wave packet, which was defined as the first point of amplitude change from the average noise level. (Figure 8) The time t = 0 corresponds to the sharp electrical pulse that drives the source transducer. It is usually referred to as the "main bang."

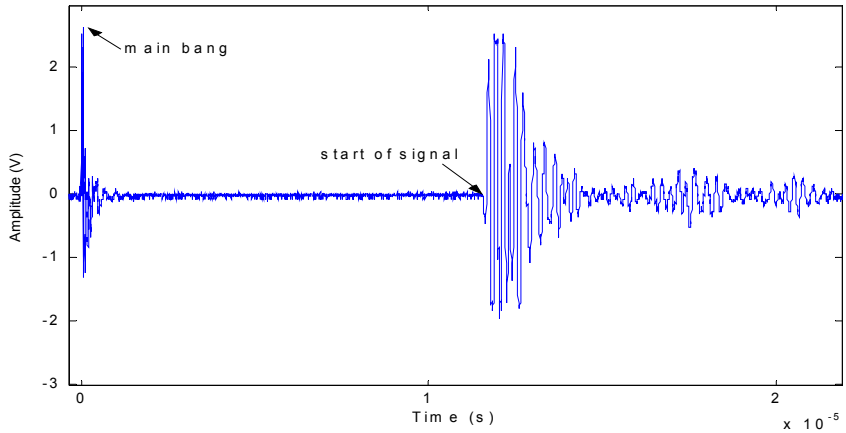


Figure 8: Sample waveform of surface wave on 20% PVA with 5MHz transducers 0.625 in (15.875 mm) apart

Other possible options included the peak of the received signal and the first zero crossing (position in which the signal crosses the x axis) of the received signal. Neither of these options was used because recorded signals of ultrasonic waves through hydrogels and cartilage did not have a consistent shape (i.e. dispersive medium) as the transducer separation distance varied. Since the shape of the received waveform did not remain the same, choosing the signal peak or the first zero crossing would have produced inconsistent time of arrival data. Using the start of the wave packet was judged to be the most consistent point on the waveform to be the time of arrival. If the surface wave

speed depended on frequency because of dispersion, taking the first arrival of the signal to determine the wave speed was therefore an upper bound on the surface wave speed.

*3.4.2 Cross correlation analysis*

Another common way to determine time of arrival is cross correlation analysis or cross spectral density analysis. Cross correlation analysis assumes that a signal represented by a time history propagates (nondispersively) a distance d at speed C. The two signals measured at a separation distance L can include some statistically independent noise. The analysis compares two continuous random processes, x(t) and y(t) and determines the time delay, $\tau$, between x(t) and y(t) using the cross correlation function given by

$$R_{xy}(\tau) = \lim_{T\to\infty} \frac{1}{T} \int_0^T x(t)y(t+\tau)dt .$$

The cross correlation coefficient $R_{xy}$ is maximum at a value of $\tau$ that corresponds to the time delay $\tau = d/C$, so that the propagation speed can be determined from the cross correlation measurement. Cross spectral density analysis is similar to cross correlation analysis, except it provides results in the frequency domain. An advantage to this method is that the propagation does not need to be nondispersive. The time delay between x(t) and y(t) is found from the phase of the spectral density function or cross spectrum, which can be defined as the Fourier transform of the correlation function between the two records:

$$S_{xy}(f) = \int_{-\infty}^{\infty} R_{xy}(\tau)e^{-i2\pi f\tau} d\tau .$$

The cross spectrum is commonly expressed in terms of a magnitude and phase angle. The phase angle is given by

$$\theta_{xy}(f) = 2\pi f \tau_1 = 2\pi f \frac{d}{c},$$

where the $\tau_1$ is the propagation time, d is a fixed distance and c is propagation velocity, which here can be a function of frequency.[62] The drawback of the cross spectral density technique is that it is necessary to unwrap the phase angle to obtain meaningful values of the wave speed. This phase unwrapping process is not trivial and the results are not always very robust. It was found that, for the data presented in this thesis, the direct time of flight (TOF) of the first arrival was the most robust method to determine the wave speed.

### ***3.5 Transducer calibration with Aluminum***

To calibrate the surface wave transducers, experiments were performed on aluminum to compare calculated surface wave speeds with known values. A pair of 5 MHz surface wave contact transducers was tested on a two inch block of aluminum with the protocol. Signals were recorded with the source and receiver transducers 0.75 in, 1 in, 1.25 in, and 1.5 in (19.05 mm, 25.4 mm, 31.75 mm, 38.1 mm) apart. From the distance versus time of arrival plot, the average wave speed was found to be 2940 m/s. The theoretically predicted Rayleigh wave speed $C_R$ in an isotropic medium is

$$C_R = \sqrt{\frac{\mu}{\rho}}\left(\frac{0.87 + 1.12\nu}{1+\nu}\right),$$

where μ is the bulk shear moduli, ρ is density, and ν is Poisson's ration. Assuming a Young's modulus of 73 GPa, Poisson's ratio of 0.33 and a density of 2800 kg/m$^3$ for

aluminum, the theoretical surface wave speed was found to be 2915 m/s. The difference between the calculated and predicted surface wave speed was 0.86%.

### ***3.6 Ultrasonic NDE testing on hydrogels: longitudinal and shear wave***

Ultrasonic NDE tests were performed using longitudinal and shear transducers to measure wave speeds through the hydrogels. The 3.524 in by 3.524 in by 0.579 in hydrogel samples were used in all ultrasonic NDE tests. To measure longitudinal and shear wave speeds, a pair of transducers were placed on opposing surfaces of the hydrogel sample, where wave travel distance was 0.579 in. (Figure 9)

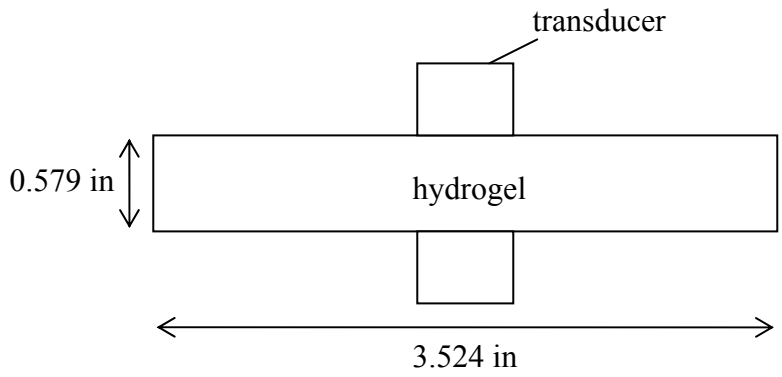


Figure 9: Experimental setup for longitudinal and shear wave speed measurements

For longitudinal wave measurements, 2.25 MHz (model A133S-RM) and 5 MHz (model A110S-RM) transducers were used. Both longitudinal transducers have a diameter of 0.24 in (6 mm). For shear wave measurements, 2.25MHz (model V154-RM) and 5MHz (model V156-RM) transducers were used. The 2.25 MHz shear transducer has a diameter of 0.512 in (13 mm) and the 5 MHz shear transducer has a diameter of 0.24 in (6 mm). Wave signals were recorded with an oscilloscope at a sampling rate of 200

MHz. Sample waveforms of a longitudinal and shear wave through hydrogels are seen in Figure 11 and Figure 12 respectively. The first main spike, commonly called the main bang, is the excitation pulse generated from the source transducer. The multiple wave packets are reflections of the waves through the thickness of the hydrogel. The received wave packet and reflections of the longitudinal wave were distinct and each reflection decreased in amplitude as expected. The received wave packet and reflections of the shear wave were also distinct, but there was a low frequency component seen in between the high frequency packets.

The time of arrival was taken to be the start of each wave packet and distance (thickness of hydrogel and its multiples) was plotted against time of arrival to find wave speeds. Sample plots of distance versus time of arrival are seen in Figure 10.

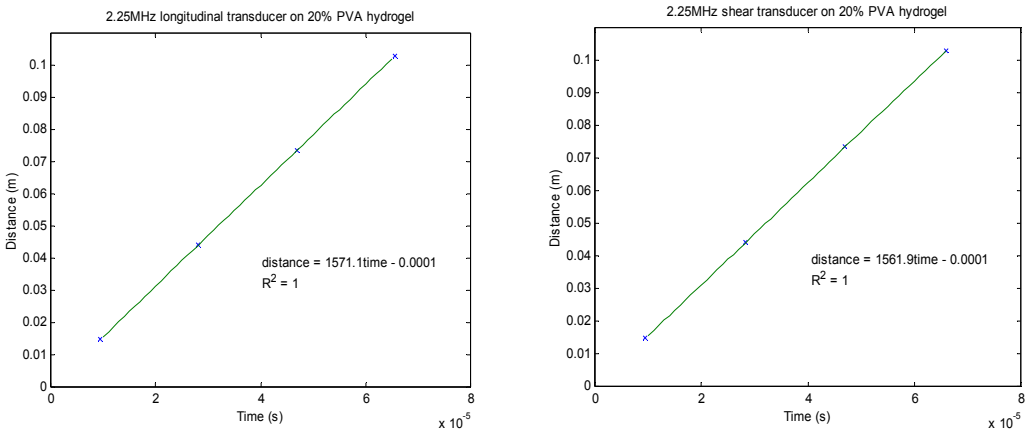


Figure 10: Sample plots of distance versus time of arrival for waves measured with longitudinal and shear transducers

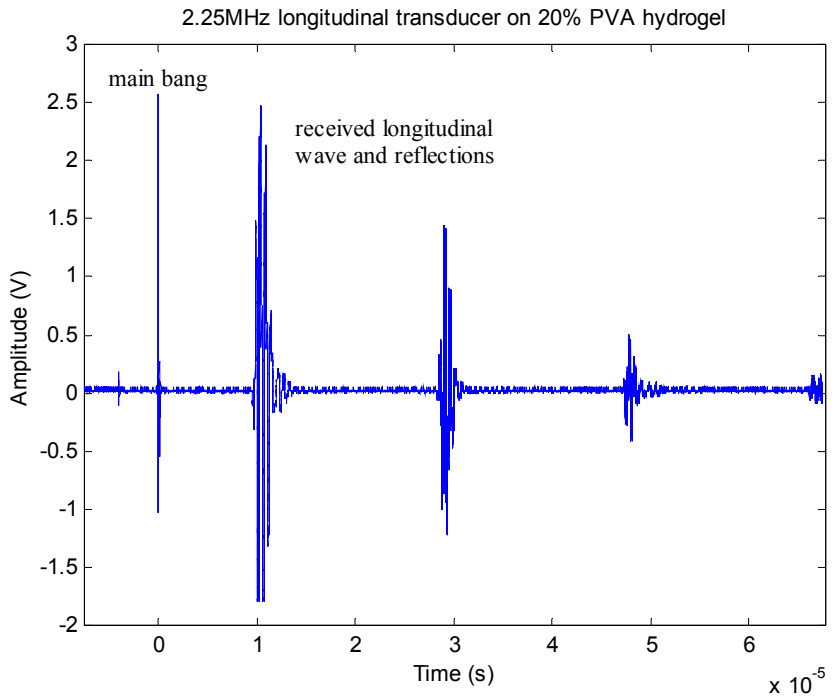


Figure 11: Sample waveform of ultrasonic longitudinal wave through a PVA hydrogel 15 mm thick

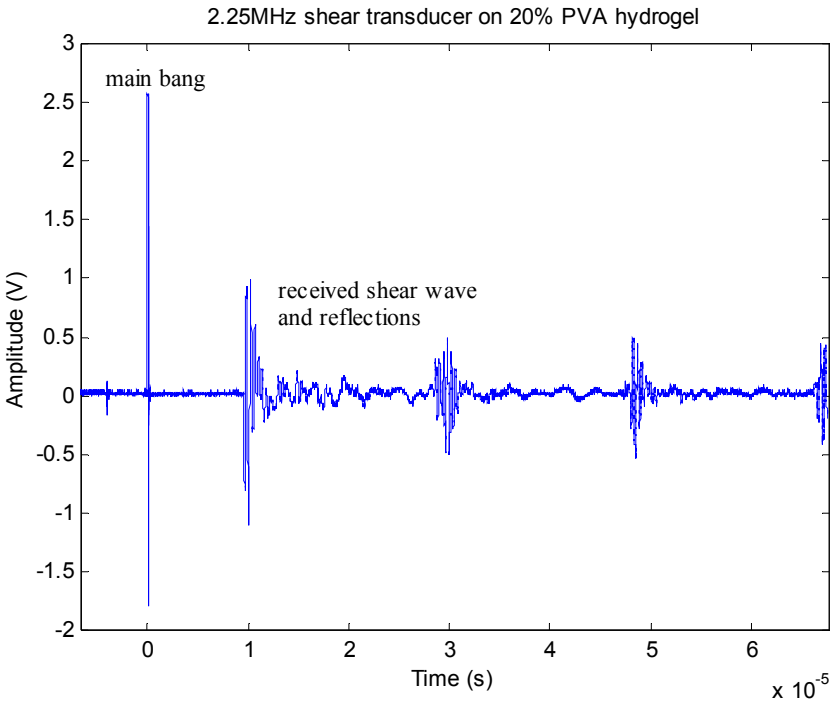


Figure 12: Sample waveform of ultrasonic shear wave through a PVA hydrogel 15 mm thick

Average wave speeds measured with longitudinal transducers are listed in Table 3 and wave speeds measured with shear transducers are listed in Table 4. For the 20% and 25% PVA with 2.25 MHz transducers, 26 longitudinal wave speeds were measured and averaged. For the 20% and 25% PVA with 5 MHz transducers, 32 longitudinal speeds were measured and averaged (Appendix B.1). For the 20% and 25% PVA with 2.25 MHz transducers, 14 shear wave speeds were measured and averaged. For the 20% and 25% PVA with 5 MHz transducers, 23 shear speeds were measured and averaged. (Appendix B.2).

Table 3: Average longitudinal wave speeds in 20% and 25% hydrogels

| PVA % | Frequency (MHz) | Average speed (m/s) | Standard Deviation (m/s) |
|---|---|---|---|
| 20 | 2.25 | 1582.22 | 37.53 |
| 20 | 5 | 1598.48 | 38.24 |
| 25 | 2.25 | 1599.99 | 31.67 |
| 25 | 5 | 1610.33 | 31.30 |

Table 4: Average shear wave speeds in 20% and 25% hydrogels

| PVA % | Frequency (MHz) | Average speed (m/s) | Standard Deviation (m/s) |
|---|---|---|---|
| 20 | 2.25 | 1591.00 | 56.93 |
| 20 | 5 | 1617.09 | 50.11 |
| 25 | 2.25 | 1595.31 | 58.48 |
| 25 | 5 | 1629.44 | 33.94 |

Using a two way ANOVA statistical analysis, it was found that the longitudinal speeds were significantly different between the 20% and 25% hydrogels ($p = 0.025$). The longitudinal speeds were also significantly different between the 2.25 and 5 MHz longitudinal transducers ($p = 0.041$). In the overall analysis, only 7.68% of the variability

was accounted for, so no conclusions could be made about longitudinal speeds in hydrogels. Using a two way ANOVA statistical analysis, it was found that the shear speeds were not significantly different between the 20% and 25% hydrogels ($p = 0.411$). The shear speeds were significantly different between the 2.25 and 5 MHz shear transducers ($p = 0.010$). In the overall analysis, only 9.4% of the variability was taken into account, thus no conclusions could be drawn about shear speeds in the hydrogels.

### ***3.7 Ultrasonic NDE testing on hydrogels: surface wave***

With the established protocol for measuring surface wave speeds, 2.25 MHz and 5MHz surface wave contact transducers were used to test the 20% and 25% hydrogels, where the samples were oriented so the thickness was 0.579 in. (Figure 13)

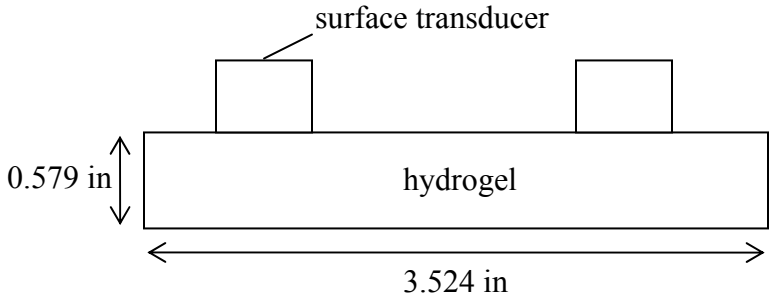


Figure 13: Experimental setup for surface wave speed measurement

Distances between source and receiver transducers ranged from 0.75 in (19.05 mm) to 2 in (50.8 mm) in 0.125 in (3.175 mm) increments. Average surface wave speeds are listed in Table 5. For the 20% and 25% PVA with 2.25 MHz transducers, 6 surface wave speeds were measured and averaged. For the 20% and 25% PVA with 5 MHz transducers, 27 surface wave speeds were measured and averaged (Appendix B.3).

Table 5: Surface wave speeds in 20% and 25% hydrogels with thickness = 15mm

| PVA % | Frequency (MHz) | Average speed (m/s) | Standard Deviation |
|---|---|---|---|
| 20 | 2.25 | 2630.47 | 299.40 |
| 20 | 5 | 2851.93 | 157.18 |
| 25 | 2.25 | 2916.70 | 125.27 |
| 25 | 5 | 2955.05 | 209.58 |

The signals recorded had multiple wave packets that increased and then decreased in amplitude as the receiver transducer moved further away from the source transducer (Figure 14).

It was discovered that surface waves were not being generated in this experiment. Since the transducer emitted a single pulse, it was hypothesized that the multiple wave packets recorded at the receiver were in fact due, at least in part, to multiple reflections. The surface wave transducers contain a built-in wedge that is optimized to excite surface waves in aluminum. The wedge is made of an acrylic resin with a longitudinal velocity of 2730 m/s and designed with an incident angle of 65°. Since the theoretical surface wave speed in aluminum is 2915 m/s, the angle of the refracted wave is 90°, or at the surface, according to Snell's law. Since the hydrogel was a softer material and thus had a slower surface wave speed, the angle of the refracted wave was less than 90°. The transducer was not generating a surface wave but a longitudinal and/or shear wave that would reflect along the thickness of the hydrogel. (Figure 15) This would explain the multiple wave packets whose amplitude increased and decreased, because the receiver transducer would detect the interfering reflections of the longitudinal and/or shear waves.

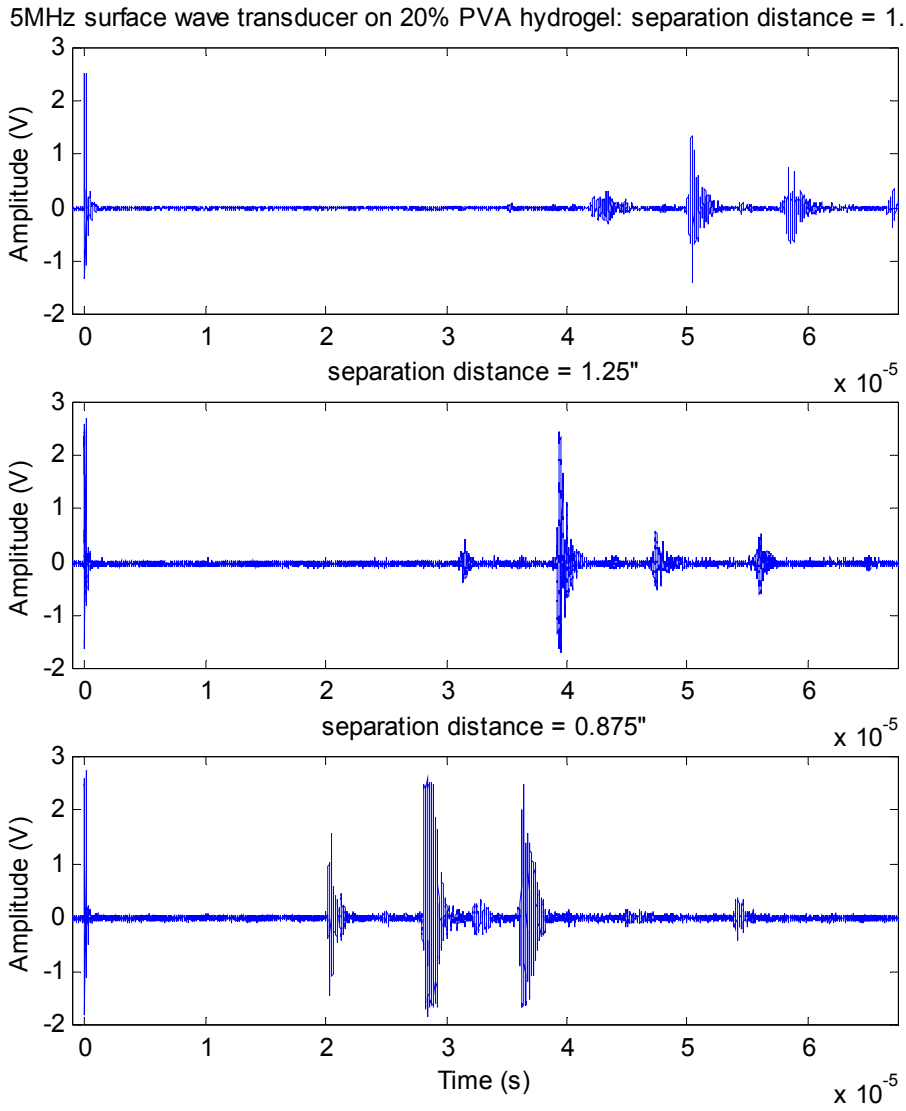


Figure 14: Sample waveform progression of ultrasonic surface wave through a PVA hydrogel 15 mm thick

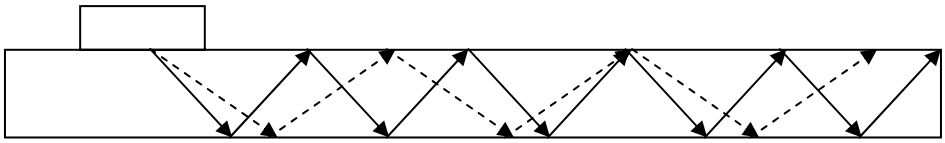

Figure 15: Reflected waves along thickness of hydrogel from surface wave contact transducer

Assuming the wave speed through the hydrogel is the shear wave speed ($C_s$ = 1591 m/s), it was calculated that the transducers were exciting a wave angled 33.40° from the vertical (see Figure 16a).

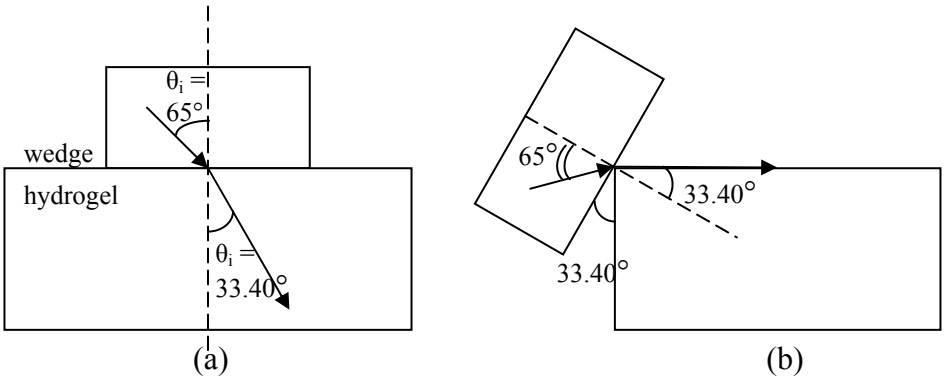


Figure 16: (a) Angle of generated wave in hydrogel with surface transducer (b) Surface transducer orientation to generated surface wave in hydrogel

According to the sample calculation, to force the excited wave to the surface, the transducer would have to be angled such that the bottom surface of the transducer is at most 33.40° from the hydrogel vertical surface as seen in Figure 16b. To simplify experimental procedure, the source transducer was oriented vertically on the corner of the hydrogel samples with the tick mark aligned with the hydrogel surface. In addition, the hydrogels were oriented where the thickness was 90 mm and distances between transducers ranged from 0.375 in (9.525 mm) to 1 in (25.4 mm) in 0.125 in (3.175 mm)

increments. If reflected waves were generated, this setup would prevent their signals from being detected (see Figure 17).

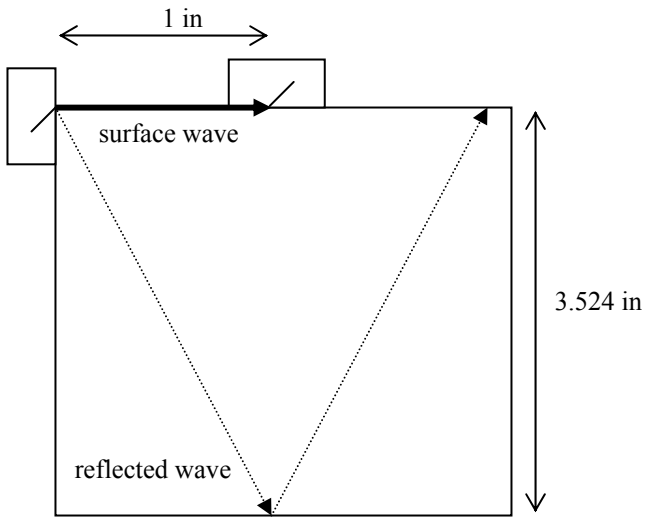


Figure 17: Experimental setup to generate surface wave in hydrogels with surface transducers

To investigate whether a surface wave could be generated, experiments were performed with the source surface transducer vertical and a 5 MHz longitudinal and shear transducer as the receiver. A signal was recorded with a longitudinal transducer as receiver and then with a shear transducer. A surface wave is composed of both longitudinal surface motion and shear surface motion. If the arrival times of both signals coincided, it indicated that the detected wave was indeed a surface wave. Time of arrivals of the first wave packet for longitudinal and shear transducers at different distances from the source transducer are listed in Table 6 and Table 7.

The differences in time of arrivals detected with longitudinal and shear transducers at the surface were all less than 5%; therefore, it can be concluded a surface wave was being generated. Surface wave speeds were then measured with 2.25 MHz and

5 MHz surface transducers, with the source transducer vertical, the hydrogel oriented with the thickness as 90 mm, and transducer distances ranged from 0.375 in (9.525 mm) to 1 in (25.4 mm) in 0.125 in (3.175 mm) increments. Recorded waveforms showed only one wave packet that decreased in amplitude as separation distance between transducers increased. (Figure 18)

Table 6: Time of arrival of signals detected by 5 MHz longitudinal and shear wave transducers at surface of 20% PVA hydrogel with source surface transducer vertically oriented

| Distance from source (m) | Time of arrival of signal detected with longitudinal transducer (s) | Time of arrival of signal detected with shear transducer (s) | % difference between longitudinal and shear wave time of arrival |
|---|---|---|---|
| 0.009525 | 5.5000e-6 | 5.7550e-6 | 4.636% |
| 0.012700 | 7.0200e-6 | 7.2750e-6 | 3.632% |
| 0.015875 | 9.0000e-6 | 9.3050e-6 | 3.389% |

Table 7: Time of arrival of signals detected by 5 MHz longitudinal and shear wave transducers at surface of 25% PVA hydrogel with source surface transducer vertically oriented

| Distance from source (m) | Time of arrival of signal detected with longitudinal transducer (s) | Time of arrival of signal detected with shear transducer (s) | % difference between longitudinal and shear wave time of arrival |
|---|---|---|---|
| 0.009525 | 5.9550e-6 | 6.0050e-6 | 0.840% |
| 0.012700 | 7.6900e-6 | 7.8400e-6 | 1.951% |
| 0.015875 | 9.3300e-6 | 9.7800e-6 | 4.823% |

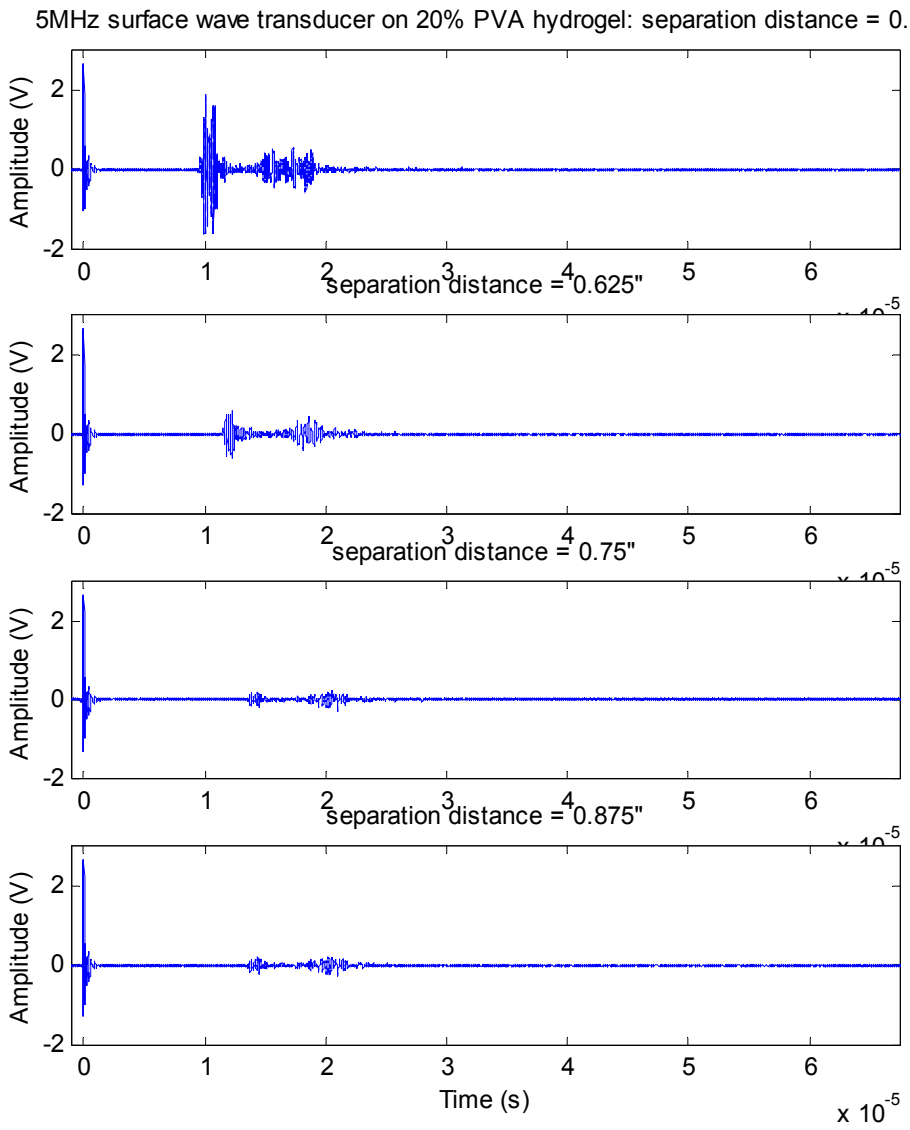


Figure 18: Sample waveform progression of ultrasonic surface wave through a PVA hydrogel 90 mm thick

Surface wave speeds in hydrogel samples oriented with the thickness 90 mm and the source transducer vertical are listed in Table 8. For the 20% and 25% PVA with 2.25 MHz transducers, 18 surface wave speeds were measured and averaged. For the 20% and 25% PVA with 5 MHz transducers, 13 surface wave speeds were measured and averaged (Appendix B.4).

Table 8: Surface wave speeds in 20% and 25% hydrogels with thickness = 90mm

| PVA % | Frequency (MHz) | Average speed (m/s) | Standard Deviation |
|---|---|---|---|
| 20 | 2.25 | 1625.52 | 68.88 |
| 20 | 5 | 1718.24 | 61.01 |
| 25 | 2.25 | 1710.79 | 48.00 |
| 25 | 5 | 1767.71 | 28.47 |

Using a two way ANOVA statistical analysis, it was found that the surface wave speeds were significantly different between the 20% and 25% hydrogels ($p < 0.0001$). The surface wave speeds were also significantly different between the 2.25 and 5 MHz surface transducers ($p < 0.0001$). In the analysis, 45.91% of the variability was taken into account. From a Tukey comparison test, the difference between average surface wave speeds on the 20% and 25% hydrogels was 71.76 m/s and the difference between average surface wave speeds with the 2.25 and 5 MHz transducer was 75.83 m/s.

Among the three types of waves propagating in a hydrogel, surface waves were faster than shear waves and longitudinal waves. In an isotropic material, the opposite occurs where the fastest waves are longitudinal waves, then shear, followed by surface wave. Because of the complex nature of hydrogels (poroelastic, two phase), acoustic behavior in hydrogels may not follow the expected trends. In fact, Feng and Johnson[63]

have shown that when the contrast in material properties between the frame and the fluid is low in a fluid saturated porous medium, the Biot theory of wave propagation in two phase media predicts that the shear wave exceeds the "slow" compressional wave. The fast compressional wave, however, always travels faster than the shear wave. It is clear that gels are soft, complex materials, and that it is difficult to measure pure compressional or shear motion at the surface by using hard PZT contact transducers.

*3.7.1 Attenuation coefficient: FFT analysis*

Consider a signal propagating in the x direction at velocity $C_R$. The signal is recorded at two positions $x_1$ and $x_2$. Assuming that attenuation dominates over other effects (such as dispersion or geometrical spreading), the signals can be expressed by

$$S(x_1,t) = e^{-\alpha x_1} f(x_1 - C_R t) \text{ and } S(x_2,t) = e^{-\alpha x_2} f(x_2 - C_R t),$$

where f() is an arbitrary pulse shape function. The frequency dependent amplitude attenuation coefficient α(f), in Neper/m, is estimated for each hydrogel sample as

$$\alpha(f) = \frac{1}{x_2 - x_1} \ln\left(\frac{\left|FFT_{x_2}(f)\right|}{\left|FFT_{x_1}(f)\right|}\right),$$

where $x_2$ and $x_1$ are different separation distances between transducers and $FFT_x$ is the FFT of the signal recorded at a distance x. At a given separation distance, hydrogel PVA concentration, and frequency, the received wave packet was extracted from the entire waveform. The extracted signal was then zero-padded to perform a 2048 point fast Fourier transform (FFT). Sample signals are shown in Figure 19.

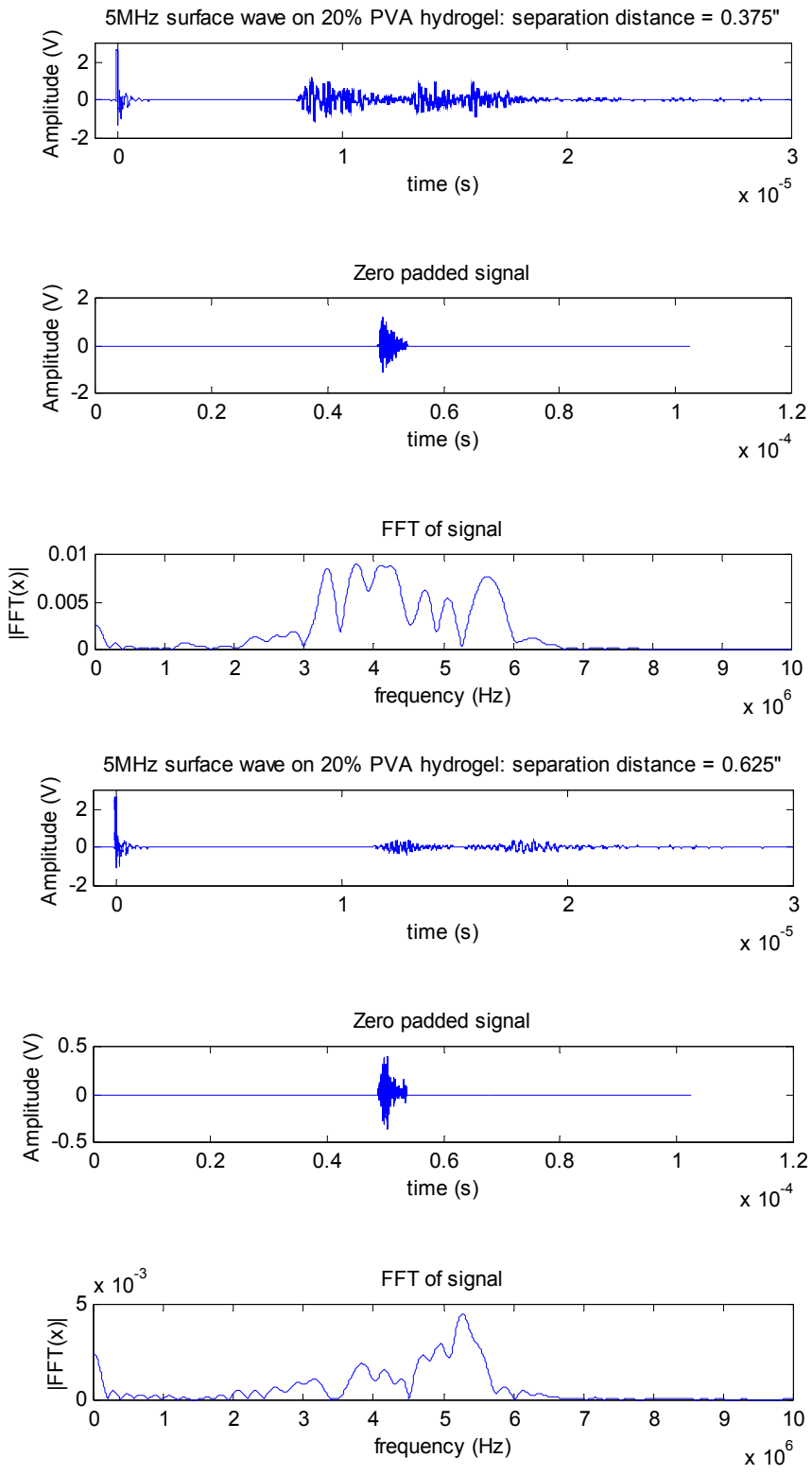


Figure 19: Sample waveforms of ultrasonic surface waves in PVA hydrogel and FFT analysis

As seen in the FFT plots, the values of the FFT amplitude drop out some frequencies near the noise level. This causes spikes in the attenuation coefficient versus frequency plot (Figure 20), which are clearly nonphysical artifacts and a meaningful attenuation factor cannot be calculated.

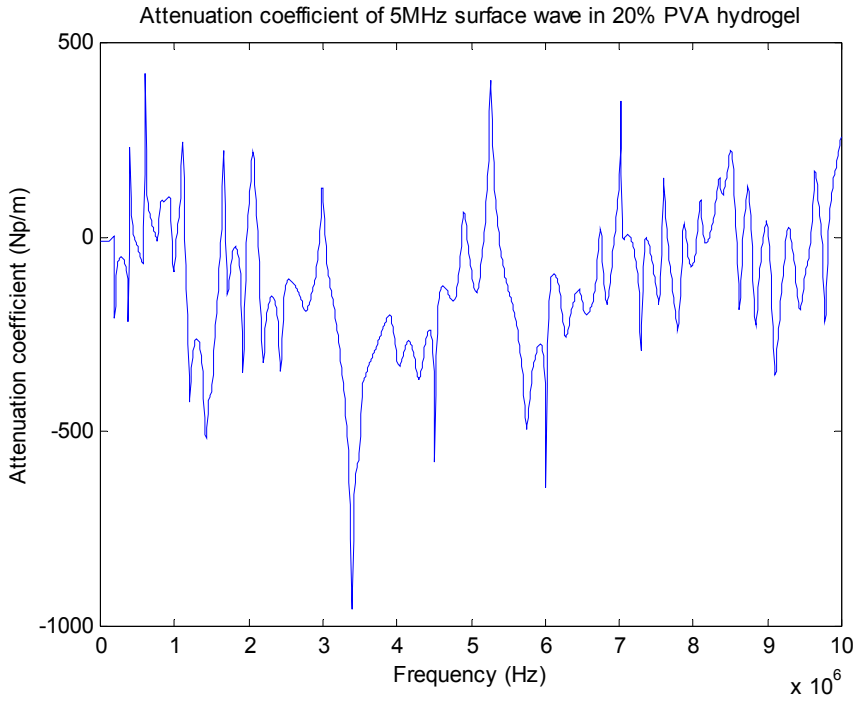


Figure 20: Sample attenuation coefficient vs frequency curve of ultrasonic surface wave in PVA hydrogel

The calculated attenuation coefficient is presented in Np/m. The conversion to change the attenuation coefficient to dB/m is given by

$$\alpha_{dB/m} = (20\log e)\alpha_{Np/m} = 8.68\alpha_{Np/m}.$$

Clearly the attenuation coefficient cannot be negative on physical grounds. The results seen in Figure 19 show that there is not enough signal to noise ratio to obtain meaningful values of the attenuation coefficient.

*3.7.2 Attenuation: RMS analysis*

Since using FFT was not successful in calculating the attenuation factor for surface waves in hydrogels, root mean square (RMS) analysis was used. The energy of a wave is proportional to the sum of the squares of the magnitudes of the waveform over a period of time. The mean square value, or $RMS^2$, for a collection of N discrete values is

$$x_{rms}^2 = \frac{1}{T}\sum_{i=0}^{N} x_i^2 * \Delta t,$$

where T is the period of the waveform and Δt is the time interval of the waveform. At a given separation distance, hydrogel PVA concentration, and frequency, the received wave packet was extracted from the entire waveform. Mean square values were calculated for the extracted waveforms of 2.25MHz and 5MHz surface waves through 20% and 25% PVA hydrogels (Table 9). Signals at two transducer separation distances were chosen for the RMS analysis. RMS values were calculated for nine signals at each distance for a particular PVA and frequency and averaged (Appendix B.5). The change in RMS values was found by calculating the difference in RMS values and dividing by the RMS value at 0.375 in.

Using a two way ANOVA statistical analysis, it was found that the RMS values were not significantly different between the 20% and 25% hydrogels ($p = 0.340$). The RMS values were also not significantly different between the 2.25 and 5 MHz surface transducers ($p = 0.247$). In the analysis, only 6.60% of the variability was taken into account, thus no conclusions could be made about the RMS values in the hydrogels.

Table 9: RMS values of 2.25 and 5MHz surface waves through 20% and 25% PVA hydrogels

| % PVA | Frequency (MHz) | Transducer separation distance (in) | Average RMS value | Standard deviation |
|---|---|---|---|---|
| 20 | 2.25 | 0.375 | 0.608 | 0.111 |
| 20 | 2.25 | 0.625 | 0.208 | 0.018 |
| **Average change in RMS values** | | | **64.8%** | **7.6%** |
| 25 | 2.25 | 0.375 | 0.716 | 0.151 |
| 25 | 2.25 | 0.625 | 0.286 | 0.023 |
| **Average change in RMS values** | | | **58.0%** | **10.9%** |
| 20 | 5 | 0.375 | 0.340 | 0.104 |
| 20 | 5 | 0.625 | 0.166 | 0.049 |
| **Average change in RMS values** | | | **46.6%** | **21.2%** |
| 25 | 5 | 0.375 | 0.500 | 0.143 |
| 25 | 5 | 0.625 | 0.175 | 0.092 |
| **Average change in RMS values** | | | **63.6%** | **16.1%** |

### ***3.8 Summary***

From dynamic shear and compression tests, it was found that the mechanical properties of the 20% and 25% hydrogels were significantly different. At 0.01 Hz, the average shear modulus of the 25% hydrogel was 143.9% higher than the average shear modulus of the 20% hydrogel. At 0.1 Hz, the average shear modulus of the 25% hydrogel was 139.3% higher than the average shear modulus of the 20% hydrogel. The average compressive modulus of the 25% hydrogel was 130.9% higher than the average compressive modulus of the 20% hydrogel.

Ultrasonic longitudinal, shear and surface wave speed measurements were found to be repeatable through hydrogels. There was little variability from sample to sample as well as over the duration of the testing period. It was found that surface waves could be generated in hydrogels by orienting the sample so the thickness was 3.54 in (90 mm) and with the source surface wave transducer vertical. Surface wave speeds of the 20% and

25% hydrogels were significantly different, which reflected the difference in mechanical properties of the hydrogels. Table 10 summarizes the results of ultrasonic wave experiments. The attenuation coefficient could not be calculated for either of the hydrogels.

Table 10: Summary of results of ultrasonic NDE tests on PVA hydrogels

| PVA % | Frequency (MHz) | Average speed measured with longitudinal transducer (st. dev.) | Average speed measured with shear transducer (st. dev.) | Average speed measured with surface transducer (st. dev.) |
|---|---|---|---|---|
| 20 | 2.25 | 1582.22 (37.53) | 1591.00 (56.93) | 1625.52 (68.88) |
| 20 | 5 | 1598.48 (38.24) | 1617.09 (50.11) | 1718.24 (61.01) |
| 25 | 2.25 | 1599.99 (31.67) | 1595.31 (58.48) | 1710.79 (48.00) |
| 25 | 5 | 1610.33 (31.30) | 1629.44 (33.94) | 1767.71 (28.47) |

# CHAPTER 4

# ULTRASONIC NDE IN ARTICULAR CARTILAGE

## *4.1 Preparation of articular cartilage*

Articular cartilage was obtained from stifle bovine joints shipped intact from Research 87 in Marlborough, MA. The tibia was separated from the joint and stored at 4°C when not being used in an experiment. During storage, the tibial plateaus were covered with phosphate buffered saline (PBS) soaked towels to keep the tissue hydrated.

## *4.2 Ultrasonic NDE testing on healthy cartilage*

The tibia was taken from the refrigerator and left at room temperature (20°C) for half an hour to allow the joint to reach room temperature. To investigate whether a surface wave could be generated through the cartilage, experiments were performed with the source surface transducer placed on the tibial plateau surface and a longitudinal or shear transducer as the receiver. The signal was recorded with a longitudinal transducer as receiver and then with a shear transducer. A surface wave is composed of both longitudinal surface motion and shear surface motion. If the arrival times of both signals coincided, it would indicate that the detected wave is indeed a surface wave. Time of arrivals for longitudinal and shear transducers at different distances from the source transducer are listed in Table 11.

The time of arrival of both the signals detected with longitudinal and shear transducers at the surface coincided, therefore suggesting a surface wave was being generated. The protocol for measuring surface wave speeds was used on the tibial

Table 11: Time of arrival of signals detected with 5 MHz longitudinal and shear wave transducers at surface of cartilage

| Distance from source (m) | Time of arrival of signal detected with longitudinal transducer (s) | Time of arrival of signal detected with shear transducer (s) | % difference between longitudinal and shear wave time of arrival |
|---|---|---|---|
| 0.012700 | 6.5250e-6 | 6.9450e-6 | 6.437% |
| 0.015875 | 8.7200e-6 | 8.4350e-6 | 3.268% |

plateaus. Surface wave speeds were calculated using 2.25 MHz surface transducers. The distances between source and receiver transducers ranged from 0.5625 in (14.288 mm) to 1.125 in (28.575 mm) in 0.1875 in (4.763 mm) increments, and the transducers were oriented in an anterior/posterior direction on the medial and lateral tibial plateaus. Recorded waveforms showed only one major wave packet that decreased in amplitude as separation distance between transducers increased. (Figure 21)

Wave speeds traveling in the anterior-posterior direction on the tibial plateaus are listed in Table 12. For the medial tibial plateau with 2.25 MHz transducers, 19 surface wave speeds were measured and averaged. For the lateral tibial plateau with 2.25 MHz transducers, 31 surface wave speeds were measured and averaged (Appendix B.6).

Table 12: Ultrasonic surface wave speeds on cartilage of bovine tibial plateaus

| Medial or lateral tibial plateau | Frequency (MHz) | Average speed (m/s) | Standard Deviation (m/s) |
|---|---|---|---|
| Medial | 2.25 | 1683.76 | 59.41 |
| Lateral | 2.25 | 1446.93 | 214.04 |

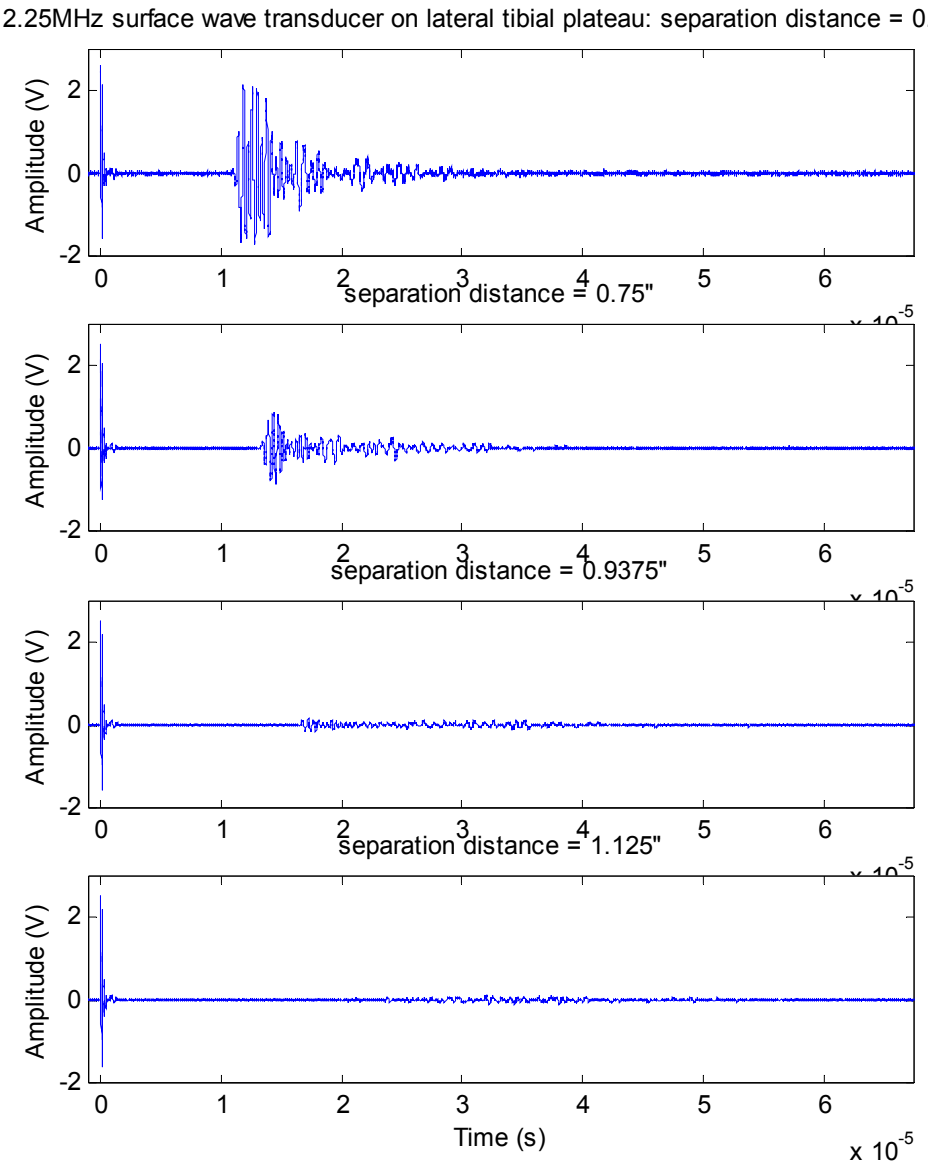


Figure 21: Sample waveform progression of ultrasonic surface wave on bovine tibia

Using a two sample t-test, it was found that the surface wave speeds were significantly different between the medial and lateral tibial plateaus ($p < 0.0001$). The medial surface wave speed was found to be 16.4% faster than the lateral surface wave speed.

Since surface waves were generated in PVA hydrogels with the source surface transducer vertical, experiments were performed on articular cartilage with the source transducer vertical to investigate whether surface waves could be generated in cartilage with this setup. The tibia was cut with a scalpel to create an edge approximately 90° from the tibial plateau surfaces so that the source transducer could be placed vertically as illustrated in Figure 22.

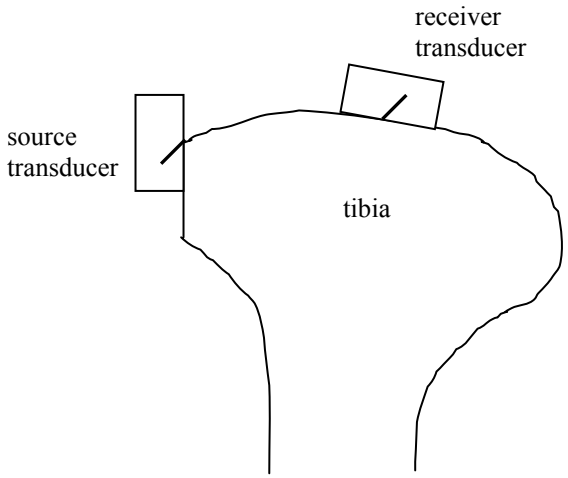


Figure 22: Side view of experimental setup for surface wave speed measurement through cartilage on tibial plateau with source transducer vertical

To determine if the generated wave was a surface wave, the signals were received first with a longitudinal and then with a shear wave transducer. Time of arrivals for

signals measured with longitudinal and shear transducers at different distances from the vertical source transducer are listed in Table 13.

Table 13: Time of arrival of signals detected by 5 MHz longitudinal and shear wave transducers at surface of cartilage with source surface transducer vertically oriented

| Distance from source (m) | Average time of arrival of signal detected with longitudinal transducer (s) | Average time of arrival of signal detected with shear transducer (s) | % difference between longitudinal and shear wave time of arrival |
|---|---|---|---|
| 0.012700 | 7.6575e-6 | 7.1925e-6 | 6.072% |
| 0.015875 | 9.4075e-6 | 9.0600e-6 | 3.694% |
| 0.019050 | 1.1345e-5 | 1.0890e-5 | 4.011% |

The time of arrival of both longitudinal and shear waves at the surface coincided, therefore, suggesting a surface wave was also being generated with this setup. Surface wave speeds were then calculated with 2.25 MHz and 5 MHz surface wave transducers, with the source transducer vertical. The distances between source and receiver transducers ranged from 0.5 in (12.7 mm) to 0.875 in (22.225 mm) in 0.125 in (3.175 mm) increments, and the transducers were oriented in an anterior/posterior direction on the medial and lateral tibial plateaus. Recorded waveforms showed signals that decreased in amplitude as separation distance between transducers increased. (Figure 23)

Surface wave speeds with the source surface transducer vertical are listed in Table 14. For the lateral and medial tibial plateau with 2.25 MHz transducers, 6 surface wave speeds were measured and averaged. For the lateral and medial tibial plateau with 5 MHz transducers, 9 surface wave speeds were measured and averaged (Appendix B.7).

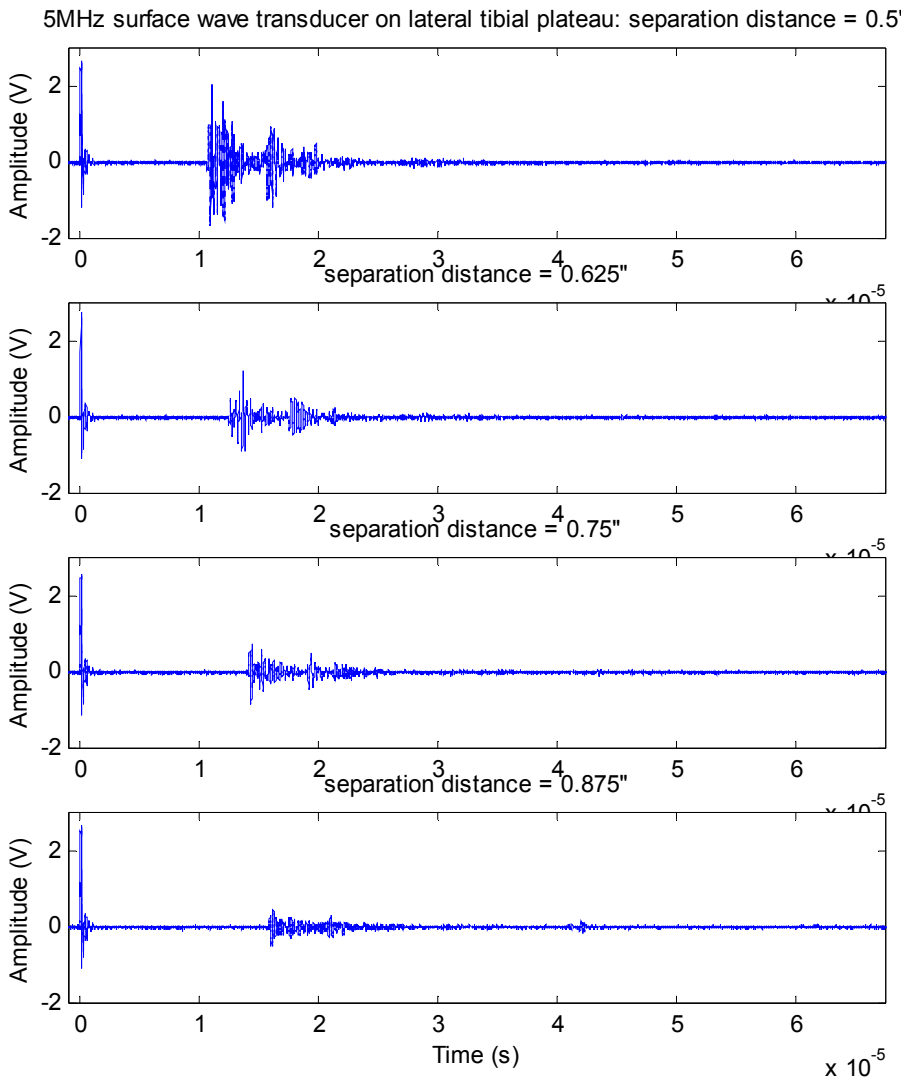


Figure 23: Sample waveform progression of ultrasonic surface wave on bovine tibia with source transducer vertical

Table 14: Surface wave speeds on cartilage of bovine tibia with source transducer vertical

| Medial or lateral tibial plateau | Frequency (MHz) | Average speed (m/s) | Standard Deviation (m/s) |
|---|---|---|---|
| medial | 2.25 | 1745.69 | 110.79 |
| medial | 5 | 1742.93 | 181.66 |
| lateral | 2.25 | 1815.28 | 102.52 |
| lateral | 5 | 1794.81 | 116.51 |

Using a two way ANOVA statistical analysis, it was found that the surface wave speeds were not significantly different between the medial and lateral tibial plateaus ($p = 0.208$). The surface wave speeds were also not significantly different between the 2.25 and 5 MHz surface transducers ($p = 0.820$). In the analysis, only 5.26% of the variability was accounted for, therefore no conclusions could be drawn about surface wave speeds on bovine tibia with the source transducer vertical.

The surface wave speeds found with the source transducer on the tibial plateau surface were comparable to the surface wave speeds found with the source transducer vertical only on the medial tibial plateau. Surface waves on the medial plateau measured with the source transducer horizontal was not significantly different from surface waves on the medial plateau measured with the source transducer vertical ($p = 0.147$), suggesting that a surface wave could be generated in bovine tibial cartilage using either experimental setup. Surface waves on the lateral plateau measured with the source transducer horizontal was significantly different from surface waves on the lateral plateau measured with the source transducer vertical ($p < 0.0001$), suggesting one of the setups did not generate a surface wave in the cartilage.

### *4.3 Ultrasonic NDE testing on damaged cartilage*

To determine the ability of surface transducers to detect changes in cartilage, tests were performed on cartilage damaged enzymatically and physically. First, cartilage on the tibial plateau was roughened with sandpaper (Al oxide grit 40). A pair of 5 MHz surface wave transducers was placed on the lateral tibial plateau, oriented in the anterior-posterior direction. The separation distance between the transducers was 0.75 in (19.05 mm) and five consecutive readings were recorded. One surface wave speed measurement was made. The surface wave speed on the abraded cartilage was 1789.61 m/s with a standard deviation of 85.13 m/s. There was no significant change in surface wave speeds between healthy cartilage and abraded cartilage tested with the same parameters ($p = 0.926$).

Since physical damage did not significantly change the surface wave speed in cartilage, cartilage was damaged with enzymatic digestion. On another joint, cartilage on the tibial plateau was damaged with trypsin, which acts to degrade proteins. A pair of 5 MHz surface wave transducers was placed on the medial tibial plateau oriented in the anterior-posterior direction 0.75 in (19.05 mm) apart. A wall of silicon sealant (DOW Corning 732 RTV multi-purpose sealant) was formed on the medial plateau around the transducers to create a well that could hold liquid. (Figure 24)

The trypsin at 0.5% at 10x was diluted 1:10 in PBS. Twenty milliliters of trypsin was placed in the well to digest the cartilage at room temperature. Wave signals were recorded every 10 minutes for 100 minutes. The trypsin was then deactivated with 20 mL of fetal bovine serum (FBS). There was no visible damage on the cartilage surface

enclosed by the silicon well. Calculated surface wave speeds during the digestion period are listed in Table 15.

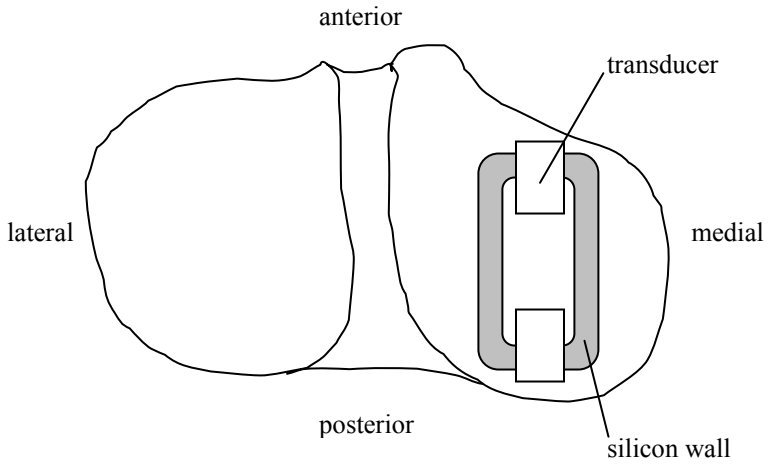


Figure 24: Experimental setup for surface wave speed measurement of trypsin digested cartilage on tibial plateau

Speeds before the 70 minute time-point were fairly constant and comparable to surface wave speeds in healthy cartilage. There was no significant change in surface wave speeds until after 70 minutes of trypsin digestion. Speeds suddenly decreased and remained constant for the remaining period of digestion. This step change in surface wave speed measurement suggests an experimental error. The silicon wall could not completely contain the trypsin, and the enzyme leaked out of the wall and underneath the transducers. Stable surface wave speed readings for 70 minutes indicate that trypsin has little effect on surface wave speed in cartilage.

To induce more detectable damage, a different enzyme was used to digest a new joint. Collagenase, which cleaves collagen strands, was used to digest the cartilage on the tibial plateau. Non-sterile 0.4% collagenase II (GIBCO lyophilized 202 units/mg)

was combined with DMEM (GIBCO 1x high glucose with L-glutamine, 110 mg 1L Na pyruvate, pyridoxine hydrochloride).

Table 15: Real time measurement of surface wave speed (5MHz transducers in anterior-posterior direction) on trypsin digested cartilage on bovine medial tibial plateau.

| Time (min) | Surface wave speed (m/s) |
|---|---|
| 0 | 1,767 |
| 10 | 1,767 |
| 20 | bad reading |
| 30 | bad reading |
| 40 | 1,770 |
| 50 | 1,769 |
| 60 | 1,770 |
| 70 | 1,779 |
| 80 | 1,526 |
| 90 | 1,526 |
| 100 | 1,526 |

The distal tibial joint was placed in a beaker containing 50 mL of collagenase digested for three hours at room temperature. After digestion, the tibial joint surfaces were rinsed with PBS. The tissue on the tibial plateaus was visibly damaged. A pair of 2.25 MHz surface wave transducers was placed on the lateral tibial plateau oriented in the anterior-posterior direction. The distances between source and receiver transducers ranged from 0.5625 in (14.2875 mm) to 1.125 in (28.575 mm) in 0.1875 in (4.7625 mm) increments. Six surface wave speed measurements were made (Appendix B.8). The average surface wave speed was found to be 1699.95 m/s with a standard deviation of 61.50 m/s. Using a two sample t-test, the digested cartilage was found to be significantly different from healthy cartilage tested with the source transducer vertical ($p = 0.046$). The speeds in the digested cartilage was lower that speeds in healthy cartilage by 115.33 m/s.

### *4.4 Summary*

It was found that ultrasonic surface waves could be generated in bovine articular cartilage with the source surface transducer horizontal and vertical relative to the surface of propagation. The surface wave speeds found with the source transducer on the tibial plateau surface were comparable to the surface wave speeds found with the source transducer vertical only on the medial tibial plateau. Surface wave speed measurements were repeatable for one sample and over the period of one day (Table 16); however, there was more variability from sample to sample and over an extended period of testing compared to hydrogels.

Surface wave speeds were measured on healthy bovine articular cartilage that was damaged physically and enzymatically. Table 17 summarizes the results of ultrasonic surface wave experiments. The surface wave speed of the abraded cartilage was not significantly different from healthy cartilage. The surface wave speed of digested cartilage was found to be significantly different from surface wave speed in healthy cartilage.

Table 16: Standard deviations in surface wave speeds in bovine articular cartilage

| Date | Sample # | Source transducer horizontal or vertical | Medial or lateral tibial plateau | Surface transducer frequency (MHz) | Standard Deviation of surface wave speed/Average wave speed |
|---|---|---|---|---|---|
| 5/19/2003 | 1 | horizontal | Medial | 2.25 | 3.507% |
| 5/20/2003 | 1 | horizontal | Medial | 2.25 | 3.418% |
| 5/21/2003 | 1 | horizontal | Medial | 2.25 | 2.777% |
| 5/29/2003 | 2 | horizontal | Lateral | 2.25 | 2.434% |
| 5/30/2003 | 2 | horizontal | Lateral | 2.25 | 3.344% |
| 5/31/2003 | 2 | horizontal | Lateral | 2.25 | 5.297% |
| 7/10/2003 | 3 | horizontal | Lateral | 2.25 | 1.699% |
| 7/11/2003 | 3 | horizontal | Lateral | 2.25 | 2.420% |
| 3/29/2004 | 5 | vertical | Medial | 2.25 | 4.976% |
| 3/30/2004 | 5 | vertical | Medial | 2.25 | 2.949% |
| 3/31/2004 | 5 | vertical | Medial | 2.25 | 6.148% |
| 3/26/2004 | 4 | vertical | Lateral | 2.25 | 6.760% |
| 3/29/2004 | 5 | vertical | Lateral | 2.25 | 5.623% |
| 3/29/2004 | 5 | vertical | Medial | 5 | 9.575% |
| 3/30/2004 | 5 | vertical | Medial | 5 | 2.723% |
| 3/31/2004 | 5 | vertical | Medial | 5 | 12.116% |
| 3/25/2004 | 4 | vertical | Lateral | 5 | 5.860% |
| 3/26/2004 | 4 | vertical | Lateral | 5 | 9.824% |
| 3/29/2004 | 5 | vertical | Lateral | 5 | 5.860% |

Table 17: Summary of results of ultrasonic NDE tests on bovine articular cartilage

| Frequency (MHz) | Medial or lateral tibial plateau | Average speed with source horizontal (st. dev.) | Average speed with source vertical (st. dev.) | Average speed of abraded cartilage (st. dev.) | Average speed of digested cartilage (st. dev.) |
|---|---|---|---|---|---|
| 2.25 | medial | 1683.76 (59.41) | 1745.69 (110.79) | - | - |
| 2.25 | lateral | 1446.93 (214.04) | 1815.28 (102.52) | - | 1699.95 (61.50) |
| 5 | medial | - | 1742.93 (181.66) | - | - |
| 5 | lateral | - | 1794.81 (116.51) | 1789.61 (85.13) | - |

# CHAPTER 5

# CONCLUSIONS AND RECOMMENDATIONS

## ***5.1 PVA hydrogels***

Hydrogels of two different PVA concentrations were prepared (20% and 25% PVA by weight) to simulate articular cartilage of different mechanical properties. Based on mechanical tests, the 25% PVA hydrogel was at least twice as stiff as the 20% PVA hydrogel in shear and compression. After validating the difference of the two gels with mechanical tests, ultrasonic NDE testing methods were used to investigate differences in mechanical properties could be detected with acoustics.

First, experiments were performed to investigate whether a surface wave could be generated in PVA hydrogels. Since the surface wave transducers were optimized to generate surface waves in aluminum, the source transducer needed to be oriented vertically with respect to the hydrogel surface of propagation. Longitudinal and shear transducers were used as receivers with the source being a vertical surface transducer. The time of arrival of signals detected by the longitudinal and shear transducers at the surface coincided, therefore suggesting a surface wave was being excited in the hydrogel.

Second, ultrasonic NDE tests were performed to test repeatability of the testing method from sample to sample as well as over the duration of a testing period. Longitudinal and shear waves at 2.25 MHz and 5 MHz were excited through the hydrogels, and measured wave speeds were found to have little variability. Surface waves at 2.25 MHz and 5 MHz were generated at the hydrogel surface, and there was little variability in the surface wave speeds. It is striking that one can measure

experimentally repeatable surface waves on hydrogels that propagate faster than the speed of sound in pure water (1500 m/s). If one were to model the gel as an isotropic homogeneous medium with density of 1055 kg/$m^3$ , a shear modulus of 75 kPa (as determined from static tests), and a Poisson ratio of 0.49 (rubber-like material), the Rayleigh wave speed would be of the order of 8 m/s. It is clear that the shear modulus at ultrasonic frequencies is much higher than that determined by quasi-static tests. In addition, PVA hydrogels are poro-viscoelastic, two phase, almost incompressible medium, containing more than 75% water. There are no existing models that adequately model the behavior of ultrasonic surface wave propagation in such a complex material.

After establishing a surface wave could be generated repeatably in hydrogels, wave speeds in the 20% and 25% PVA hydrogels were compared. The coefficient of variation was less than 10% in the analysis of longitudinal and shear wave speeds in the hydrogels. No distinct differences could be made in bulk wave speeds in 20% and 25% hydrogels. It appears that, either due to the finite size of the transducers or to the nature of the gel itself, waves generated by longitudinal or shear transducers may not be purely longitudinal or shear plane waves but a complex combination of both types of waves. The average surface wave speed measured with a 2.25 MHz transducer is 1625.52 m/s in a 20% gel and 1718.24 m/s in a 25% gel. The average surface wave speed measured with a 5 MHz transducer is 1710.79 m/s in a 20% gel and 1767.71 m/s in a 25% gel. The higher speeds in the 25% PVA hydrogels suggest ultrasonic surface wave speeds increase in materials with stiffer mechanical properties. The surface wave speeds between the 20% and 25% hydrogel were significantly different ($p < 0.001$), therefore indicating

ultrasonic NDE with surface waves could be used to detect differences in material properties of a synthetic biomaterial.

RMS analysis was used to calculate attenuation in hydrogels, but no significant differences were seen. The lack of a distinct difference of surface wave energy loss in the 20% and 25% PVA hydrogel may be caused by the couplant used on the transducers or any fluid on the hydrogel surface. The amplitude was highly sensitive to the amount of couplant or fluid on the surface of propagation. With more fluid, the signal amplitude increased. The couplant also caused the water in the hydrogel to diffuse onto the surface, thus increasing the amount of fluid on the testing surface and dehydrating the gel. The amount of couplant used and amount of fluid on the hydrogel surface was difficult to control which would lead to wave signals with inconsistent amplitudes and difficulty in attenuation coefficient calculations.

A limitation of the experimental arrangement used in this thesis was that contact, PZT (hard material) transducers were used to generate and detect Rayleigh waves on soft viscoelastic materials such as PVA and articular cartilage. These transducers are designed to generate surface waves in elastically stiff materials, such as steel and aluminum. It was thus necessary to experiment with the angular positioning of the transducers to generate a surface wave. Longitudinal and shear transducers were used to detect signals from a source surface transducer. The time of arrivals detected by the receiving transducers coincided, which led to the conclusion that a surface wave was produced; however, a non-contact laser interferometer operating at ultrasonic frequencies would be a more reliable detection system to validate that a surface wave is indeed being generated. It was found also that, with the current experimental method which relied on contact

transducers, it was difficult to measure amplitude attenuation of surface waves and relate it in a meaningful way to material properties of the surface layer. Again, it is possible that one could overcome that difficulty with non-contact laser ultrasonics.

### ***5.2 Articular cartilage***

After establishing that surface wave generation in PVA hydrogels was possible, ultrasonic NDE tests with surface waves were performed on articular cartilage of a bovine tibia. First, experiments were performed to determine whether a surface wave could be generated in articular cartilage. The source surface wave transducer was placed on the tibial plateau surface, and longitudinal and shear wave transducers were used as receivers. The time of arrival of signals recorded with longitudinal and shear transducers coincided, indicating that a surface wave was being generated on the cartilage surface. Since surface waves were generated on PVA hydrogels with the source surface transducer vertical, the tibial joint was cut to create a surface vertical to the tibial plateaus. The source surface transducer was placed on the vertical surface and the receiver was a longitudinal or shear transducer. The time of arrival of signals recorded with longitudinal and shear transducers coincided, indicating a surface wave could also be generated with this setup. Surface wave speeds measured with both setups were comparable, which also suggests that surface waves could be generated with the source transducer horizontal or vertical.

Next, experiments were performed to test repeatability of ultrasonic NDE from sample to sample and over the duration of a testing period. A pair of surface wave transducers was placed on the articulating surface of the tibial plateau to measure surface wave speeds. The surface wave speeds calculated were repeatable with consecutive

experiments over a period of two hours; however, the experiments were not repeatable over several days. Surface wave speeds varied from day to day without any monotonic trends. There were also sample to sample variations and variability from medial to lateral tibial plateaus. Surface wave speeds were then measured on the articular cartilage with the source oriented vertically relative to the tibial surface. Surface wave speeds measured with this setup had less variability. The calculated speeds were repeatable from sample to sample as well as over a period of several days.

Surface wave speeds were measured on cartilage damaged mechanically and enzymatically and compared to speeds in healthy cartilage. There was no significant change in surface wave speeds between healthy cartilage and abraded cartilage tested with the same parameters ($p = 0.926$). Presumably, the main effect of the sandpaper was to change the thickness of the cartilage more than its mechanical properties. For cartilage digested with trypsin, there was no significant change in surface wave speeds until after 70 minutes of trypsin digestion. Speeds suddenly decreased and remained constant for the remaining period of digestion, which suggests an experimental setup error. The stability of surface speed measurements for the first 70 minutes of digestion indicates that trypsin had little effect on surface wave speed. Cartilage digested with trypsin may not have been damaged since the enzyme was not operating at its optimal temperature. Surface wave speeds on cartilage digested with collagenase were significantly different from speeds on healthy cartilage ($p = 0.046$); however, the lack of structural integrity of the cartilage after digestion prevented accurate placement and repeatable contact area of the contact transducers. The digested layer of cartilage would be pushed out from underneath the transducer when the transducer was placed on the cartilage. It was

difficult to determine if the surface wave was propagating through the digested cartilage or the layer of undigested cartilage underneath.

### ***5.3 Future work***

Initial experiments have demonstrated proof of concept that ultrasonic NDE testing methods using surface wave speeds is possible on cartilage and hydrogels, a model material for cartilage. Surface waves can be repeatably generated using contact transducers in hydrogels, and wave speeds do reflect the different material properties of hydrogels. In cartilage, surface waves can also be generated with cartilage though with less repeatability. There were several factors that may be the source of the variability. Cartilage is a biological tissue that likely degraded over time. Also, cartilage is sensitive to environmental factors such as temperature and humidity that could not be controlled in this experimental setup. The main factor affecting surface wave speed variability was the physical limitations of the contact transducers. The curvature of the tibial plateau in two directions was large relative to the contact area of the surface wave transducers. Placing the transducer at the same point of contact on the tibial plateau was very difficult. Since the surface wave was very sensitive to the transducer placement and positioning, the inability to consistently place the transducers on the tibial plateau at various distances introduced variability to the surface wave speed calculations.

For future work, a better system and procedure need to be developed to ensure repeatability in wave speed measurement. To have consistent area of contact between transducers and the cartilage sample, smaller contact transducers could be used. Another possibility is to use laser generated ultrasound with sufficient low energy density so that there is no localized damage at the surface at the generation spot.[64] A laser Doppler

vibrometer (LDV) with ultrasonic frequency range could then be used for non-contact detection of the surface wave. To eliminate variability from environmental factors, experiments could be performed in an enclosed system that could maintain constant temperature and humidity. An accurate positioning system is needed to eliminate error of measuring distances between the source of wave generation and the wave detector.

Once surface wave speed measurement in healthy cartilage is repeatable, surface wave speed measurements need to be performed on damaged cartilage to test the sensitivity of ultrasonic NDE tests to changes in material properties of biological tissue. Enzymatic digestion of cartilage needs to be optimized such that there is sufficient damage that can be repeatably detected, while the integrity of the tissue is maintained.

APPENDIX A: Rayleigh waves on curved surfaces

Rayleigh wave velocity on a curved surface, c, is given by

$$c = c_o(1+\eta), \qquad \eta = a_u \frac{1}{k_o \rho_u} + a_v \frac{1}{k_o \rho_v}$$

where $c_o$ is the Rayleigh wave velocity on a plane surface, $k_o$ is the Rayleigh wave number for a plane surface, and $a_u$ and $a_v$ are given by

$$a_u = -\frac{A}{2B}, \qquad a_v = -\frac{G}{2B}.$$

The constants A, B and G are given by

$$A = \frac{l_o^2 q_o}{s_o^2 k_o} + \frac{p_o^2 s_o}{q_o^2 k_o} - 4\left(\frac{s_o}{k_o} + \frac{q_o}{k_o}\right) - \left(2 - \frac{k_t^2}{k_o^2}\right)\left[\left(\frac{k_t^2}{k_l^2} - 2\right)\frac{q_o}{k_o} - \frac{s_o}{k_o}\right],$$

$$B = 4\left(2 - \frac{k_t^2}{k_o^2}\right) - 4q_o s_o\left(\frac{1}{2s_o^2} + \frac{1}{2q_o^2} + \frac{1}{k_o^2}\right),$$

$$G = \left(\frac{k_t^2}{k_o^2} - 2\right)\left[\frac{s_o}{k_o} + \frac{q_o}{k_o}\left(\frac{k_t^2}{k_l^2} - 2\right)\right],$$

where $k_o$ is the Rayleigh wave number for a plane surface, $k_t$ is the transverse wave number, and $k_l$ is the longitudinal wave number, $q_o^2$ is $k_o^2 - k_l^2$, $s_o^2$ is $k_o^2 - k_t^2$, $p_o^2$ is $k_o^2 + k_l^2$, $l_o^2$ is $k_o^2 + k_t^2$.[53]

APPENDIX B: Raw data

## ***B.1 Speeds measured with longitudinal contact transducers on hydrogels***

Table 18: Speeds measured with 2.25 MHz longitudinal transducer on PVA hydrogels

| Date | Run | Speed in 20% PVA (m/s) | Speed in 25% PVA (m/s) |
|---|---|---|---|
| 12/4/03 | 1 | 1525.7 | |
| | 2 | 1576.7 | |
| | 3 | 1562.7 | |
| | 4 | 1562.1 | |
| 12/5/03 | 1 | | 1571.5 |
| | 2 | | 1591.7 |
| | 3 | | 1562.6 |
| | 4 | | 1575.6 |
| 1/17/04 | 1 | 1647.7 | 1718.8 |
| | 2 | 1693.9 | 1671.5 |
| 1/30/04 | 1 | 1625.8 | 1580.1 |
| | 2 | 1631.2 | 1623.2 |
| | 3 | 1632.7 | 1577.2 |
| | 4 | 1526.1 | 1586.1 |
| 2/4/04 | 1 | 1576.8 | 1594.1 |
| | 2 | 1567.5 | 1589.8 |
| | 3 | 1544.7 | 1594.9 |
| | 4 | 1563.2 | 1596.2 |
| 2/5/04 | 1 | 1577.9 | 1577.2 |
| | 2 | 1587.7 | 1587.1 |
| | 3 | 1578.3 | 1594.9 |
| | 4 | 1565.0 | 1601.7 |
| 2/6/04 | 1 | 1584.5 | 1611.6 |
| | 2 | 1546.5 | 1604.1 |
| | 3 | 1577.4 | 1604.4 |
| | 4 | 1587.5 | 1602.1 |
| 2/7/04 | 1 | 1557.7 | 1585.6 |
| | 2 | 1571.1 | 1599.6 |
| | 3 | 1582.9 | 1603.7 |
| | 4 | 1584.5 | 1594.5 |

Table 19: Speeds measured with 5 MHz longitudinal transducer on PVA hydrogels

| Date | Run | Speed in 20% PVA (m/s) | Speed in 25% PVA (m/s) |
|---|---|---|---|
| 9/18/03 | 1 | 1,563.2 | 1,603.5 |
| | 2 | 1,553.3 | 1,591.5 |
| | 3 | 1,581.2 | 1,604.3 |
| | 4 | 1,581.2 | 1,632.4 |
| | 5 | 1,578.8 | 1,624.9 |
| | 6 | 1,575.7 | 1,631.6 |
| 10/29/03 | 1 | | 1562.8 |
| | 2 | | 1561.3 |
| | 3 | | 1594.3 |
| | 4 | | 1593.7 |
| 12/4/03 | 1 | 1592.1 | |
| | 2 | 1600.9 | |
| | 3 | 1606.6 | |
| | 4 | 1599.6 | |
| 12/5/03 | 1 | | 1592.5 |
| | 2 | | 1607.8 |
| | 3 | | 1584.7 |
| | 4 | | 1616.0 |
| 1/17/04 | 1 | 1669.1 | 1740.4 |
| | 2 | 1731.9 | 1675.4 |
| 1/30/04 | 1 | 1630.7 | 1645.1 |
| | 2 | 1607.2 | 1595.8 |
| | 3 | 1506.4 | 1591.6 |
| | 4 | 1623.2 | |
| 2/4/04 | 1 | 1588.3 | 1607.6 |
| | 2 | 1583.8 | 1618.7 |
| | 3 | 1598.5 | 1615.2 |
| | 4 | 1583.8 | 1631.5 |
| 2/5/04 | 1 | 1612.5 | 1598.1 |
| | 2 | 1557.5 | 1615.2 |
| | 3 | 1550.2 | 1595.4 |
| | 4 | 1613.3 | 1611.0 |
| 2/6/04 | 1 | 1632.4 | 1612.0 |
| | 2 | 1602.8 | 1608.5 |
| | 3 | 1616.6 | 1610.2 |
| | 4 | 1623.0 | 1623.2 |
| 2/7/04 | 1 | 1588.0 | 1587.1 |
| | 2 | 1611.0 | 1593.1 |
| | 3 | 1600.3 | 1592.1 |
| | 4 | 1588.4 | 1593.1 |

***B.2 Speeds measured with shear contact transducers on hydrogels***

Table 20: Speeds measured with 2.25 MHz shear transducer on PVA hydrogels

| Date | Run | Speed in 20% PVA (m/s) | Speed in 25% PVA (m/s) |
|---|---|---|---|
| 1/17/04 | 1 | 1697.8 | 1704.8 |
| | 2 | 1760.6 | 1754.1 |
| 2/5/04 | 1 | 1579.8 | 1585.4 |
| | 2 | 1571.9 | 1583.4 |
| | 3 | 1577.2 | 1569.8 |
| | 4 | 1554.9 | 1569.2 |
| 2/6/04 | 1 | 1555.5 | 1586.8 |
| | 2 | 1560.3 | 1584.8 |
| | 3 | 1558.3 | 1569.1 |
| | 4 | 1574.0 | 1581.3 |
| 2/7/04 | 1 | 1557.2 | 1564.0 |
| | 2 | 1552.0 | 1560.6 |
| | 3 | 1561.9 | 1563.8 |
| | 4 | 1554.6 | 1557.3 |

Table 21: Speeds measured with 5 MHz shear transducer on PVA hydrogels

| Date | Run | Speed in 20% PVA (m/s) | Speed in 25% PVA (m/s) |
|---|---|---|---|
| 9/18/03 | 1 | 1616.6 | 1668.3 |
| | 2 | 1606.8 | 1666.7 |
| | 3 | 1692.4 | 1649.8 |
| | 4 | 1692.4 | 1645.1 |
| | 5 | 1605.2 | 1694.0 |
| | 6 | 1621.6 | 1623.9 |
| 10/29/03 | 1 | | 1636.9 |
| | 2 | | 1630.1 |
| | 3 | | 1632.0 |
| 12/4/03 | 1 | 1621.5 | |
| | 2 | 1625.1 | |
| 1/5/04 | 1 | 1659.0 | |
| | 2 | 1653.0 | |
| 1/17/04 | 1 | 1725.2 | 1725.2 |
| | 2 | 1730.8 | 1639.1 |
| 2/5/04 | 1 | 1593.3 | 1618.2 |
| | 2 | 1588.2 | 1618.3 |
| | 3 | 1593.5 | 1617.6 |
| | 4 | 1580.4 | 1597.8 |
| 2/6/04 | 1 | 1564.2 | 1621.6 |
| | 2 | 1598.3 | 1600.6 |
| | 3 | 1588.8 | 1607.1 |
| | 4 | 1560.2 | 1597.8 |
| 2/7/04 | 1 | 1580.6 | 1608.5 |
| | 2 | 1577.1 | 1591.3 |
| | 3 | 1576.2 | 1592.8 |
| | 4 | 1559.7 | 1594.3 |

***B.3 Speeds measured with surface contact transducers on hydrogels (thickness = 15mm)***

Table 22: Speeds measured with 2.25 MHz surface contact transducers on PVA hydrogels with thickness = 15 mm

| Date | Run | Speed in 20% PVA (m/s) | Speed in 25% PVA (m/s) |
|---|---|---|---|
| 10/2/03 | 1 | 2485.5 | |
| | 2 | 2398.4 | |
| | 3 | 2768.3 | |
| | 4 | 2464.5 | 2983.0 |
| | 5 | 2550.2 | 3054.9 |
| | 6 | 3255.4 | 2955.7 |
| 10/3/03 | 1 | | 2870.0 |
| | 2 | | 2692.0 |
| | 3 | | 2944.6 |

Table 23: Speeds measured with 5 MHz surface contact transducers on PVA hydrogels with thickness = 15 mm

| Date | Run | Speed in 20% PVA (m/s) | Speed in 25% PVA (m/s) |
|---|---|---|---|
| 8/14/03 | 1 | 2759.0 | 2934.6 |
| | 2 | 2743.3 | 2991.2 |
| | 3 | | 2921.8 |
| | 4 | | 2983.5 |
| | 5 | | 2899.8 |
| 8/18/03 | 1 | 2689.2 | 2891.4 |
| | 2 | 2680.8 | 2923.6 |
| | 3 | 2718.6 | 2888.9 |
| 8/19/03 | 1 | 2797.2 | 2796.5 |
| | 2 | 2845.0 | 3005.1 |
| | 3 | 2865.4 | 2839.3 |
| 8/20/03 | 1 | 2861.8 | 2842.5 |
| | 2 | 2780.7 | 2874.0 |
| | 3 | 2752.2 | 2868.6 |
| 8/21/03 | 1 | 3208.5 | 2862.4 |
| | 2 | 2953.4 | 2876.6 |
| | 3 | 3031.3 | 2899.2 |
| 8/26/03 | 1 | 2868.6 | 2829.7 |
| | 2 | 2832.2 | 2832.0 |
| | 3 | 2716.0 | 2847.2 |
| 9/29/03 | 1 | 3180.6 | 3388.6 |
| | 2 | 3129.8 | 3550.0 |
| | 3 | 3077.3 | |
| 9/30/03 | 1 | 2707.9 | 3591.4 |
| | 2 | 2880.5 | 2752.7 |
| | 3 | 2681.2 | 3205.4 |
| 10/29/03 | 1 | | 2783.4 |
| | 2 | | 2807.5 |
| 11/19/03 | 1 | | 2974.2 |
| | 2 | | 3144.7 |
| | 3 | | 3009.5 |
| | 4 | | 2624.4 |
| 12/4/03 | 1 | 2850.6 | |

***B.4 Speeds measured with surface contact transducers on hydrogels (thickness = 90 mm)***

Table 24: Speeds measured with 2.25 MHz surface contact transducers on PVA hydrogels with thickness = 90 mm

| Date | Run | Speed in 20% PVA (m/s) | Speed in 25% PVA (m/s) |
|---|---|---|---|
| 2/12/04 | 1 | 1,710.4 | 1,748.9 |
| | 2 | 1,756.9 | 1,715.2 |
| | 3 | 1,683.9 | 1,802.3 |
| 2/16/04 | 1 | 1,605.9 | 1,793.8 |
| | 2 | 1,636.4 | 1,765.5 |
| | 3 | 1,616.3 | 1,746.1 |
| 2/17/04 | 1 | 1,519.1 | 1,679.7 |
| | 2 | 1,653.2 | 1,610.5 |
| | 3 | 1,439.9 | 1,658.6 |
| 2/18/04 | 1 | 1,641.8 | 1,711.9 |
| | 2 | 1,649.4 | 1,681.1 |
| | 3 | 1,597.0 | 1,720.5 |
| 2/19/04 | 1 | 1,591.6 | 1,676.8 |
| | 2 | 1,605.0 | 1,693.7 |
| | 3 | 1,601.8 | 1,670.6 |
| 2/20/04 | 1 | 1,649.2 | 1,711.5 |
| | 2 | 1,654.8 | 1,716.0 |
| | 3 | 1,646.8 | 1,691.6 |

Table 25: Speeds measured with 5 MHz surface contact transducers on PVA hydrogels with thickness = 90 mm

| Date | Run | Speed in 20% PVA (m/s) | Speed in 25% PVA (m/s) |
|---|---|---|---|
| 1/2/04 | 1 | 1,816.8 | |
| | 2 | 1,783.5 | 1811.6 |
| 1/5/04 | 1 | 1844.3 | |
| 2/12/04 | 1 | 1,677.2 | 1,803.6 |
| | 2 | 1,703.4 | 1,779.4 |
| | 3 | 1,678.5 | 1,774.1 |
| 2/16/04 | 1 | 1,696.7 | 1,791.2 |
| | 2 | 1,655.3 | 1,735.2 |
| | 3 | 1,681.0 | 1,744.7 |
| 2/17/04 | 1 | 1,696.6 | 1,756.5 |
| | 2 | 1,689.9 | 1,731.8 |
| | 3 | 1,695.7 | 1,749.0 |

***B.5 RMS values of waves generated with surface wave contact transducers on hydrogels***

Table 26: RMS values of signals measured with 2.25 MHz surface contact transducers on PVA hydrogels

| Date | Run | RMS value in 20% PVA at 0.375 in. | RMS value in 20% PVA at 0.625 in. | % difference of RMS value |
|---|---|---|---|---|
| 2/18/04 | 1 | 0.585089 | 0.217566 | 62.81% |
| | 2 | 0.585971 | 0.208034 | 64.50% |
| | 3 | 0.642881 | 0.216499 | 66.32% |
| 2/19/04 | 1 | 0.456613 | 0.226891 | 50.31% |
| | 2 | 0.477212 | 0.204291 | 57.19% |
| | 3 | 0.756377 | 0.230964 | 69.46% |
| 2/20/04 | 1 | 0.632716 | 0.174768 | 72.38% |
| | 2 | 0.784055 | 0.195392 | 75.08% |
| | 3 | 0.552301 | 0.194494 | 64.78% |
| Date | Run | RMS value in 25% PVA at 0.375 in. | RMS value in 25% PVA at 0.625 in. | % difference of RMS value |
| 2/18/04 | 1 | 0.849597 | 0.333679 | 60.73% |
| | 2 | 0.767765 | 0.290483 | 62.17% |
| | 3 | 0.818021 | 0.259825 | 68.24% |
| 2/19/04 | 1 | 0.769275 | 0.271641 | 64.69% |
| | 2 | 0.730443 | 0.299583 | 58.99% |
| | 3 | 0.803874 | 0.290194 | 63.90% |
| 2/20/04 | 1 | 0.772178 | 0.285798 | 62.99% |
| | 2 | 0.388039 | 0.256406 | 33.92% |
| | 3 | 0.541829 | 0.290470 | 46.39% |

Table 27: RMS values of signals measured with 5 MHz surface contact transducers on PVA hydrogels

| Date | Run | RMS value in 20% PVA at 0.375 in. | RMS value in 20% PVA at 0.625 in. | % difference of RMS value |
|---|---|---|---|---|
| 2/18/04 | 1 | 0.367689 | 0.114884 | 68.76% |
| | 2 | 0.349044 | 0.159416 | 54.33% |
| | 3 | 0.308783 | 0.121120 | 60.78% |
| 2/19/04 | 1 | 0.319736 | 0.219097 | 31.48% |
| | 2 | 0.294238 | 0.207628 | 29.44% |
| | 3 | 0.437631 | 0.226402 | 48.27% |
| 2/20/04 | 1 | 0.282164 | 0.203946 | 27.72% |
| | 2 | 0.535927 | 0.104447 | 80.51% |
| | 3 | 0.162375 | 0.132695 | 18.28% |
| Date | Run | RMS value in 25% PVA at 0.375 in. | RMS value in 25% PVA at 0.625 in. | % difference of RMS value |
| 2/18/04 | 1 | 0.347613 | 0.137054 | 60.57% |
| | 2 | 0.667337 | 0.113385 | 83.01% |
| | 3 | 0.466786 | 0.144938 | 68.95% |
| 2/19/04 | 1 | 0.583405 | 0.318338 | 45.43% |
| | 2 | 0.588761 | 0.242189 | 58.86% |
| | 3 | 0.509255 | 0.312786 | 38.58% |
| 2/20/04 | 1 | 0.296113 | 0.121210 | 59.07% |
| | 2 | 0.348028 | 0.104932 | 69.85% |
| | 3 | 0.675065 | 0.077972 | 88.45% |

***B.6 Speeds measured with surface wave contact transducers on bovine articular cartilage***

Table 28: Speeds measured with 2.25 MHz surface contact transducers on the tibial plateau of bovine cartilage

| Date | Run | Speed in lateral tibial plateau (m/s) | Speed in medial tibial plateau (m/s) |
|---|---|---|---|
| 2/20/03 | 1 | 1643.5 | 1707.8 |
| 5/29/03 | 1 | 1248.6 | 1553.6 |
| | 2 | 1245.3 | 1672.8 |
| | 3 | 1225.7 | 1622.0 |
| | 4 | 1204.4 | 1650.5 |
| | 5 | 1201.4 | 1622.7 |
| | 6 | 1171.1 | 1725.4 |
| 5/30/03 | 1 | 1150.5 | 1675.3 |
| | 2 | 1158.6 | 1622.6 |
| | 3 | 1197.8 | 1737.3 |
| | 4 | 1211.5 | 1779.4 |
| | 5 | 1235.8 | 1762.1 |
| | 6 | 1249.8 | 1733.4 |
| 5/31/03 | 1 | 1381.2 | 1694.7 |
| | 2 | 1566.0 | 1667.0 |
| | 3 | 1413.4 | 1627.8 |
| | 4 | 1412.8 | 1660.9 |
| | 5 | 1543.9 | 1761.8 |
| | 6 | 1429.1 | 1714.3 |
| 7/10/03 | 1 | 1566.6 | |
| | 2 | 1642.4 | |
| | 3 | 1623.2 | |
| | 4 | 1618.2 | |
| | 5 | 1591.8 | |
| | 6 | 1625.9 | |
| 7/11/03 | 1 | 1740.0 | |
| | 2 | 1698.4 | |
| | 3 | 1654.7 | |
| | 4 | 1778.7 | |
| | 5 | 1709.2 | |
| | 6 | 1715.4 | |

***B.7 Speeds measured with surface wave contact transducers vertical on bovine articular cartilage***

Table 29: Speeds measured with 2.25 MHz surface contact transducers vertical on the tibial plateau of bovine cartilage

| Date | Run | Speed in lateral tibial plateau (m/s) | Speed in medial tibial plateau (m/s) |
|---|---|---|---|
| 3/29/04 | 1 | 1692.0 | 1938.4 |
| | 2 | 1870.4 | 1801.8 |
| | 3 | 1929.8 | 1765.1 |
| 3/30/04 | 1 | 1704.6 | 1755.8 |
| | 2 | 1788.8 | 1707.8 |
| | 3 | 1906.1 | 1811.4 |

Table 30: Speeds measured with 5 MHz surface contact transducers vertical on the tibial plateau of bovine cartilage

| Date | Run | Speed in lateral tibial plateau (m/s) | Speed in medial tibial plateau (m/s) |
|---|---|---|---|
| 3/26/04 | 1 | 1930.7 | 1745.6 |
| | 2 | 1753.1 | 1450.5 |
| | 3 | 1741.7 | 1684.6 |
| 3/29/04 | 1 | 1963.2 | 1847.4 |
| | 2 | 1632.1 | 1948.0 |
| | 3 | 1707.0 | 1919.6 |
| 3/30/04 | 1 | 1930.7 | 1653.3 |
| | 2 | 1753.1 | 1920.8 |
| | 3 | 1741.7 | 1516.6 |

***B.7 Speeds measured with surface wave contact transducers on digested bovine articular cartilage***

Table 31: Speeds measured with 2.25 MHz surface contact transducers on bovine cartilage digested with 0.4% collagenase II

| Date | Run | Speed in lateral tibial plateau (m/s) |
|---|---|---|
| 7/11/03 | 1 | 1650.0 |
| | 2 | 1675.5 |
| | 3 | 1627.0 |
| | 4 | 1751.1 |
| | 5 | 1788.4 |
| | 6 | 1707.7 |

# REFERENCES


[1] Buckwalter, J.A. and V.C. Mow, "Cartilage repair in osteoarthritis," in Osteoarthritis: Diagnosis and Medical/Surgical Management, 2nd Ed. (R.W. Moskowitz, D.S. Howell, V.C. Goldberg, H.J. Mankins, eds.), Philadelphia, W.B. Saunders Company, pp 71-107, 1992.

[2] Nagy, P. B. Introduction to Ultrasonics, Course notes, University of Cincinnati, 2001.

[3] Mow, V.C. and A. Ratcliffe, "Structure and function of articular cartilage and meniscus," in Basic Orthopaedic Biomechanics, 2nd Ed. (V.C. Mow and W.C. Hayes, eds.), Philadelphia, Lippincott-Raven, pp113-178, 1997.

[4] Knudson, C.B. and W. Knudson, "Cartilage proteoglycans," Semin. Cell Dev. Biol., 12: 69-78 (2001).

[5] Bodine, A.J., Brown N., Hayes, W.C. and S.A. Jiminez, "The effect of sodium chloride on the shear modulus of articular cartilage," Trans ORS, 5:137 (1980).

[6] Soltz, M.A. and G.A. Ateshian, "Interstitial fluid pressurization during confined compression cyclical loading of articular cartilage," Ann. Biomed. Eng, 28:150-159 (2000).

[7] Hunziker, E.B. Michel, M., and D. Studer, "Ultrastructure of adult human cartilage matrix after cryotechnical processing," Microsc. Res. Tech., 37:271-284 (1997).

[8] Venn, M. and A. Maroudas, "Chemical composition and swelling of normal and osteoarthritic femoral head cartilage. I. Chemical composition," Ann. Rheum. Dis., 36: 121-129 (1977).

[9] Korhonen, R.K., Wong, M., Arokoski, J., Lindgren, R., Helminen, H.J., Hunziker, E.B. and J.S. Jurvelin, "Importance of the superficial tissue layer for the indentation stiffness of articular cartilage," Med. Eng. Phys., 24:99-108 (2002).

[10] Jeffrey, A.K., Blunn, G.W., Archer, C.W. and G. Bentley, "Three-dimensional collagen architecture in bovine articular cartilage," J. Bone Joint Surg. Br., 73:795-801 (1991).

[11] Arokoski, J.P., Hyttinen, M.M., Helminen, H.J. and J.S. Jurvelin, "Biomechanical and structural characteristics of canine femoral and tibial cartilage," J. Biomed. Mater. Res., 48:99-107 (1999).

[12] Torzilli, P.A., Dethmers, D.A., rose, D.E. and H.F. Schryuer, "Movement of interstitial water through loaded articular cartilage," Journal of Biomechanics, 16:169-179 (1983).

[13] Schinagl, R.M., Gurskis, D., Chen, A.C. and R. L. Sah, "Depth-dependent confined compression modulus of full thickness bovine articular cartilage,' Journal of Orthopaedic Research, 15:499-506 (1997).

[14] Athanasiou, K.A., Rosenwasser, M.P., Buckwalter, J.A., Malinin, T.I. and V.C. Mow, "Interspecies comparison of in situ mechanical properties of distal femoral cartilage," Journal of Orthopaedic Research, 9:330-349 (1991).

[15] Mow, V.C., Gibbs, M.C., Lai, W.M., Zhu, W.B., and K.A. Athanasiou, "Biphasic indentation of articular cartilage-II. A numerical algorithm and an experimental study," Journal of Biomechanics, 22:853-861 (1989).

[16] Jurvelin, J., Kiviranta, I., Sammanen, A.M., Tammi, M. and H.J. Helminen, "Indentation stiffness of young canine articular cartilage – influence of strenuous joint loading," Journal of Biomechanics, 23:1239-1246 (1990).

[17] Hayes, W.C and A.J. Bodine, "Flow independent viscoelastic properties of articular cartilage matrix," Journal of Biomechanics, 11:407-419 (1978).

[18] Zhu, W.B., Lai, W.M., and V.C. Mow, "Intrinsic quasilinear viscoelastic behaviour of the extracellular matrix of cartilage," Trans. Orthop. Res. Soc., 11:407 (1986).

[19] Setton, L.A., Mow, V.C., and D.S. Howell, "The mechanical behavior of articular cartilage in shear is altered by transaction of the anterior cruciate ligament," Journal of Orthopaedic Research, 13:473-482 (1995).

[20] Akizuki, S., Mow, V.C., Muller, F., Pita, J.C., Howell, D.S. and D.H. Manicourt, "Tensile properties of human knee joint cartilage: I. Influence of ionic concentrations, weight bearing, and fibrillation on the tensile modulus," Journal of Orthopaedic Research, 5:173-186 (1987).

[21] Ebara, S., Kekar, R., Bigliani, L.U., Pollock, R.G., Pwluk, R.P., Flatow, E.L., Ratcliffe, A., and V.C. Mow, "Bovine glenoid cartilage is less stiff than humeral head cartilage in tension," Trans Orthop Res Soc.,19:146 (1994).

[22] Setton, L.A., Mow, V.C., Muller, F.J., Pita, J.C., and D.S. Howell, "Mechanical properties of canine articular cartilage are significantly altered following transaction of the anterior cruciate ligament," Journal of Orthopaedic Research, 12:451-463 (1994).

[23]Chiang, E.H., Laing, T.J., Meyer, C.R., Boes, J.L., Rubin, J.M. and R.S. Adler, "Ultrasonic characterization of in vitro osteoarthritic articular cartilage with validation by confocal microscopy," Ultrasound in Medicine and Biology, 23 (2):205-213 (1997).
[24] Fife, R.S., "Osteoarthritis: Epidemiology, pathology and pathogenesis," in Primer on the Rheumatic Diseases, 11th Ed. (J.H. Klippel, C.M. Weyand, and R.L. Wortmann, eds.), Atlanta, Arthritis Foundation, pp 216-218, 1997.

[25] Hochberg, M.C., "Osteoarthritis: Clinical features and treatments," in Primer on the Rheumatic Diseases, 11th Ed. (J.H. Klippel, C.M. Weyand, and R.L. Wortmann, eds.), Atlanta, Arthritis Foundation, pp 216-218, 1997.

[26] Nuki, G., "Osteoarthritis: a problem of joint failure," S. Rheumatol., 58:142-147 (1999).

[27] Okada, Y., "Matrix-degrading mealloproteinases and their roles in joint destruction," Mod. Rheumatology, 10:121-128 (2000).

[28] Guilak, F., Ratcliffe, A., Lane, N., Rosenwasser, M.P., and V.C. Mow, "Mechanical and biomechanical changes in the superficial zone of articular cartilage in canine experimental osteoarthritis," Journal of Orthopedic Research, 12:474-484 (1994).

[29] Akizuki, S., Mow, V.C., Muller, F., Pita, J.C., Howell, D.S., and D.H. Manicourt, "Tensile properties of human knee joint cartilage: I. Influence of ionic conditions, weight bearing, and fibrillation on the tensile modulus," Journal of Orthopedic Research, 4:379-393 (1986).

[30] Triantafillopoulos, I.K., Papgelopoulos, P.J., Politi, P.K. and A. Nikiforidis, "Articular changes in experimentally induced patellar trauma," Knee. Surg. Sports Tramatol. Arthosc., 10:144-153 (2002).

[31] Kimura, T., Nakata, K., Tsumaki, N., Miyamoto, S., Matsui, Y., Ebara, S., and T. Ochi, "Progressive degeneration of articular cartilage and intervertebral discs. An experimental study in transgenic mice bearing a type IX collagen mutation," Int. Orthop., 20:177-181 (1996).

[32] Price, J.S., Till, S.H., Bickerstaff, D.R., Bayliss, M.T., and A.P. Hollander, "Degradation of cartilage type II collagen precedes the onset of osteoarthritis following anterior cruciate ligament rupture," Arthritis Rheumatology, 42:2390-2398 (1999).

[33] Narmoneva, D.A., Wang, J.Y., and L.A. Setton, "A noncontacting method for material property determination for articular cartilage from osmotic loading," Biophys. J., 81:3066-3076 (2001).

[34] Fuente, F.R., "Electromechanical Indentation Properties of Hydrated Biomaterials," M.S. Thesis, Georgia Institute of Technology (2001).

[35] Agemura, D.H. and W.D. O'Brien, "Ultrasonic propagation properties of articular cartilage at 100MHz," Journal of the Acoustical Society of America, 87(4):1786-1791 (1990).

[36] Pellaumail, B., Dewailly, V., Watrin, A., Loeuille, D., Netter, P., Berger, G., and A. Saied, "Attenuation coefficient and speed of sound in immature and mature rat cartilage: a study in the 30-70 MHz frequency range," IEEE Ultrasonics Symposium, 1361-1466 (1999).

[37] Nieminen, H.J., Toyras, J., Rieppo, J., Nieminen, M.T., Hirvonen, J., Korhonen, R., and J.S. Jurvelin, "Real-time ultrasound analysis of articular cartilage degradation in vitro," Ultrasound in Medicine and Biology, 28(4):519-525 (2002).

[38] Toyras, J., Rieppo, J., Nieminen, M.T., Helminen, H.J., and J.S. Jurvelin, "Characterization of enzymatically induced degradation of articular cartilage using high frequency ultrasound," Phys. Med. Biol., 44:2723-2733 (1999).

[39] Senzig, D.A. and F.K. Forster, "Ultrasonic attenuation in articular cartilage," Journal of the Acoustical Society of America, 92(2):676-681 (1992).

[40] Viktorov, I. Rayleigh and Lamb Waves (Plenum Press, New York; 1967).

[41] Tolstoy, I. Wave Propagation, (McGraw Hill, New York; 1973).

[42] Lee, J.J., Stokoe, K.H., McNerney, M.T. and B.F. McCullogh, "In-situ evaluation of layer stiffnesses in airport pavements by crosshole seismic tests," Trans. Res. Rec., 1639:62-72 (1998).

[43] Scott, W., Larson, G., Martin, J., and P. Rogers, "Seismic/electromagnetic system for landmine detection," Journal of the Acoustical Society of America,107:2897 (2000).

[44] Cook, D. and Y.H. Berthelot, "Detection of small surface-breaking fatigue cracks in steel using scattering of Rayleigh waves," NDT&E Intl., 34:483-492 (2001).

[45] Chimenti, D. and O. Lobkis, "The effect of rough surfaces on guided waves," Ultrasonics, 36:155-162 (1998).

[46] Chimenti, D., "Guided waves and their use in material characterization," Appl. Mech. Rev., 50:247-284 (1997).

[47] Biryukov, S.V., Gulyaev, Y.V., Krylov, V.V., and V.P. Plessky, "Surface Acoustic Waves in Inhomogeneous Media," in Wave Phenomena (L.M. Brekhovskikh, L.B. Felsen, and H.A. Haus, eds.), Berlin, Springer-Verlag, pp 196-203, 1992.

[48] Destrade, M., "Surface waves in orthotropic incompressible materials," Journal of the Acoustical Society of America, 110(2):837-840 (2001).

[49] Ogden, R.W. and P.C. Vinh, "On Rayleigh waves in incompressible orthotropic elastic solids," Journal of the Acoustical Society of America, 115(2):530-533 (2004).

[50] Royer, D. and E. Dieulesaint, "Rayleigh wave velocity and displacement in orthorhombic, tetragonal, hexagonal, and cubic crystals," Journal of the Acoustical Society of America, 76(5):1438-1444 (1984).

[51] Kikuchi, H., Sakai, K., and K. Takagi, "Complex propagation of surface waves on soft gels," The American Physical Society, 49(5):3061-3065 (1994).

[52] Matsuoka, T., Kinouchi, W., Shinobu, K., and N. Hiroyasu, "Surface wave velocity of crosslinked polyacrylate gels," Japanese Journal of applied Physics, 38(5b):3105-3106 (1999).

[53] Takashi, H. and P.K. Choi, "Sol-Gel transition in gelatin observed with surface waves," Japanese Journal of Applied Physics, 35:2939-2943 (1996).

[54] Hoffman, A.S., "Hydrogels for biomedical applications," Advanced Drug Delivery Reviews, 43:3-12 (2002).

[55] Peppas, N.A., "Characterization of homogeneous and pseudocomposite homopolymers and copolymers for articular cartilage replacement," Biomat. Med. Div. Art. Org., 7(3):421-433 (1979).

[56] Peppas, N.A. and E.W. Merril, "Development of a semi-crystalline poly(vinyl alcohol) for biomedical applications," J. Biomed. Mater. Research, 11:423-434 (1977).

[57] Corkhill, P.H., Fitton, J.H., and B.J. Tighe, "Towards a synthetic articular cartilage," Journal of Biomaterial Science Polymer Edition, 4:615-630 (1993).

[58] Sawae, Y., Murakami, T., Higaki, H., and S. Moriyama, "Lubrication Properties of Total Knee Prostheses with PVA Hydrogel Layer as Artificial Cartilage," JSME International Journal, Series C, 39:356-364 (1996).

[59] Murikami, T., Higaki, H., Sawae, Y., Ohtsuki, N., Moriyama, S., and Y. Nakanishi, "Adaptive multimode lubrication in natural synovial joints and artificial joints," Proc. Institution Mech. Engrs., Part H, 212:23-35 (1998).

[60] Gu, Z.Q., Xiao, J.M., and X. H. Zhang, "The development of artificial articular cartilage – PVA hydrogel," Biomedical Materials and Engineering, 8:75-81 (1998).

[61] Stammen, J.A., Williams, S., Ku, D.N., and R.E. Guldberg, "Mechanical Properties of a novel PVA hydrogel in shear and unconfined compression," Biomaterials, 22:799-806 (2001).

[62] Bendat, J.S. and A.G. Piersol, Engineering Applications of Correlation and Spectral Analysis, (John Wiley and Sons, New York;1980).

[63] Feng, S. and D.L. Johnson, "High frequency acoustic properties of a fluid/porous solid interface. I. New surface mode," Journal of the Acoustical Society of America, 74(3):906-914 (1983).

[64] Scruby, C.B. and L.E. Drain, Laser Ultrasonics: Techniques and Applications (Adam Hilger; New York; 1990).